AEDC-TR-66-111

FLOW FIELD AND SURFACE PRESSURE MEASUREMENTS IN THE FULLY MERGED AND TRANSITION FLOW REGIMES ON A COOLED SHARP FLAT PLATE

Manfred Becker and David E. Boylan

ARO, Inc.

September 1966

VON KÁRMÁN GAS DYNAMICS FACILITY
ARNOLD ENGINEERING DEVELOPMENT CENTER
AIR FORCE SYSTEMS COMMAND
ARNOLD AIR FORCE STATION, TENNESSEE

NOTICES

When U. S. Government drawings specifications, or other data are used for any purpose other than a definitely related Government procurement operation, the Government thereby incurs no responsibility nor any obligation whatsoever, and the fact that the Government may have formulated, furnished, or in any way supplied the said drawings, specifications, or other data, is not to be regarded by implication or otherwise, or in any manner licensing the holder or any other person or corporation, or conveying any rights or permission to manufacture, use, or sell any patented invention that may in any way be related thereto.

Qualified users may obtain copies of this report from the Defense Documentation Center.

References to named commercial products in this report are not to be considered in any sense as an endorsement of the product by the United States Air Force or the Government.

FLOW FIELD AND SURFACE PRESSURE MEASUREMENTS IN THE FULLY MERGED AND TRANSITION FLOW REGIMES ON A COOLED SHARP FLAT PLATE

Manfred Becker and David E. Boylan
ARO, Inc.

AF - AEDC
Arnold AFS Tenn

FOREWORD

The research reported herein was done at the request of the Arnold Engineering Development Center (AEDC), Air Force Systems Command (AFSC), under Program Element 62405334, Project 8953, Task 895306.

The results of research presented were obtained by ARO, Inc. (a subsidiary of Sverdrup & Parcel and Associates, Inc.), contract operator of AEDC, AFSC, Arnold Air Force Station, Tennessee, under Contract AF 40(600)-1200. The research was conducted under ARO Project VL2517 while the senior author (an employee of the German Defense Ministry) was temporarily assigned to AEDC by the Department of Defense. The research was conducted from October 1964 to December 1965, and the manuscript was submitted for publication on May 10, 1965.

The information reported herein was also presented as a paper at the Fifth International Symposium on Rarefied Gas Dynamics, Oxford, England, July 4-8, 1966.

The authors wish to acknowledge the assistance of J. L. Potter who suggested the investigation and aided in the analysis of the results.

This technical report has been reviewed and is approved.

Larry R. Walter
Captain, USAF
Analysis Division
Directorate of Plans and Technology

Donald D. Carlson
Colonel, USAF
Director of Plans and Technology

ABSTRACT

The experimental survey of the flow field near the leading edge of a cooled, sharp flat plate parallel to a hypersonic stream of low density is discussed. Results consisting of impact pressure and hot-wire anemometer profiles plus surface pressures are analyzed and compared to recent theoretical results. Data are presented for viscous interaction parameters, $M_\infty(C_\infty/Re_\infty)^{1/2}$, as high as 2.0.

CONTENTS

ILLUSTRATIONS

TABLES

NOMENCLATURE

C	Constant
C_p	Pressure coefficient $(p_w - p_\infty)/q_\infty$
C_∞	Chapman-Rubesin constant $(\mu_w T_\infty)/(\mu_\infty T_w)$
D	Constant
D_i	Inner diameter
D_o	Outer diameter
L	Length
M_∞	Freestream Mach number
N	Number of collisions required for zero slip
n	Shock slope, $y - x^n$
p_w	Wall surface pressure
$(p_w/p_\infty)_{FM}$	Free-molecular flow limit
p_o	Tunnel stagnation pressure
p_∞	Freestream static pressure
$p_{\infty, o} = p'_o$	Stagnation pressure measured behind a normal shock in the freestream
$p_{2, o}$	Stagnation pressure measured in the shock layer (See Fig. 3)
q_∞	Freestream dynamic pressure $(\rho_\infty/2)u_\infty^2$
R_{wi}	Wire resistance
$R_{wi, \infty}$	Wire resistance in freestream
Re_∞	Unit Reynolds number
$Re_{\infty, x}$	Reynolds number based on distance x from leading edge
S_∞	Freestream speed ratio
T	Temperature
T_o	Tunnel stagnation temperature
T_w/T_o	Ratio of wall to stagnation temperature
t	Leading-edge bluntness
u_∞	Freestream velocity

$\bar{v}_{\infty, x}$	Viscous interaction parameter $M_\infty (C_\infty/Re_{\infty, x})^{1/2}$
x	Distance from leading edge
y	Distance normal to surface of the flat plate
y_A	Actual outer edge of the shock (see Fig. 5)
y'_A	Defined shock boundary determined by the maximum slope (see Fig. 5)
y_B	Peak of measured profile (see Fig. 5)
y_{ms}	Height above the surface of the flat plate to the middle of the shock (Δ_{ms})
α	Wedge angle at the leading edge (on the surface not being surveyed)
Δ_{ms}	Shock thickness determined by maximum slope
δ^*	Boundary-layer displacement thickness
ϵ	Density ratio
θ	Shock angle
λ_∞	Freestream mean free path (based on a static gas billiard ball model)
μ_∞	Freestream coefficient of viscosity
ζ	Slip parameter, $M_\infty \lambda_\infty N$
ρ_∞	Freestream density
$\bar{\chi}_{\infty, x}$	Strong interaction parameter, $\bar{v}_{\infty, x} (M_\infty)^2$

SUBSCRIPTS

1, 2	Regions in the viscous shock layer in front of and behind a normal shock (see Fig. 3)
S	Slip conditions
w	Wall value
∞	Freestream (see Fig. 3)

SECTION I
INTRODUCTION

The determination of the flow field near the leading edge of a semi-infinite flat plate in a hypersonic stream has received a considerable amount of attention in recent years. For application to practical situations, such as the re-entry of winged vehicles, the cold-wall case with $T_W/T_O \ll 1$ appears to be of the most interest. Thus, the present discussion is limited largely to the cold-wall condition. Available experimental studies are discussed in detail in conjunction with the present results in later sections.

A typical schematic of the flow over the surface of a sharp flat plate in hypersonic rarefied flow is shown in Fig. 1. A comprehensive discussion of the weak and strong interaction regimes is given by Hayes and Probstein (Ref. 1). It is generally recognized that strong interaction theory fails to predict the behavior of the flow very near the leading edge, and the determination of the actual point of departure from strong interaction was a primary consideration in the present investigation. The flow upstream of this point may be broadly divided into the merged-layer, transition, and near-free-molecular flow regimes. The merged and transition regimes have been studied by Oguchi (Refs. 2 and 3), Laurmann (Ref. 4), Talbot (Ref. 5), Jain and Li (Ref. 6), Pan and Probstein (Ref. 7), Garvine (Ref. 8), and Chow (Ref. 9). Near-free-molecular flow has been studied by Charwat (Ref. 10), Kogan (Ref. 11), and Bird (Ref. 12). The free-molecular limit is discussed in Hayes and Probstein (Ref. 1).

The local surface measurements of pressure, heat transfer, and skin friction have been used to test the accuracy of the various theoretical approaches. One obvious difference may be noted in comparing available theoretical analyses in regard to predicted surface pressure distributions. The results of Oguchi (Refs. 2 and 3) and Jain and Li (Ref. 6) predict a pressure plateau to exist over a substantial portion of the plate before a fall to the free-molecular flow limit. The results of Pan and Probstein (Ref. 7) indicate a pressure peak similar to the heat-transfer results. In the near-free-molecular flow regime, Charwat (Ref. 10) predicts the existence of a pressure plateau beginning downstream of the leading edge, whereas Kogan (Ref. 11) and Bird (Ref. 12) suggest that, even very close to the leading edge, no region of true free-molecular flow will exist.

It was felt that an experimental study which could clarify the shock and viscous layer structure and determine accurately the surface pressure

distribution might offer a substantial improvement in the basic understanding of the flow. Also, experimental work appears to be necessary before the boundaries of the various flow regimes, and therefore the matching points of the theoretical studies, can be determined.

The facility utilized by the present authors is capable of producing continuous, hypersonic, low-density flow containing no axial or lateral gradients in the test region. The flow is sufficiently rarefied to allow local pressure and flow field surveys to be conducted in the fully merged flow regime. To be explicit, the data were obtained in the range $0.1 \lesssim \bar{v}_{\infty, x} \lesssim 2.0$, where $\bar{v}_{\infty, x}$ is the viscous interaction parameter defined as

$$\bar{v}_{\infty, x} = M_{\infty} (C_{\infty}/Re_{\infty, x})^{1/2}$$

Measurements include impact pressure probe and hot-wire anemometer surveys through the shock layer, and static pressure measurements at the surface of the plate.

SECTION II
APPARATUS

The data were obtained using the arc-heated, low-density hypersonic tunnel (Gas Dynamic Wind Tunnel, Hypersonic (L)) located at the von Kármán Gas Dynamics Facility (VKF), Arnold Engineering Development Center (AEDC), Air Force Systems Command (AFSC), USAF, Arnold Air Force Station, Tennessee.

2.1 WIND TUNNEL

Tunnel L, shown in Fig. 2, is a low-density, hypersonic, continuous-type, arc-heated, ejector-pumped facility, normally using nitrogen or argon as the test gas and consisting of the following major components, in streamwise order:

1. Continuous, water-cooled, d-c arc heater, Thermal Dynamic F-40 or U-50, both modified slightly, with a 40-kw selenium rectifier power supply. Gas is injected without swirl in the F-40 arc heater and with or without swirl in the U-50 unit. Unless otherwise noted, all testing is done without use of swirling gas injection.
2. Cylindrical, water-cooled settling section of variable size, but normally of 3-in. diameter and 6- to 10-in. length.

3. Axisymmetric, aerodynamic nozzle, variable sizes with 0.10- to 1.20-in. -diam throats and 2.0- to 8.2-in. -diam exits. Four contoured nozzles having no flow gradients in the test section are currently available, in addition to older conical nozzles.
4. Cylindrical test section tank of 48-in. diameter surrounding the test section and containing instrumentation, cooling water connections, and probe carrier.
5. Axisymmetric diffuser with interchangeable designs for varying test conditions, convergent entrance, constant-area throat, divergent exit sections, and water-cooled entrance.
6. Water-cooled heat exchanger
7. Isolation valve
8. Air ejector of two stages
9. Connection to the VKF, evacuated, 200,000-cu-ft, spherical vacuum reservoir and its pumping system.

All critical components of the tunnel and related system are protected by backside water cooling. The two-stage ejector system is driven by air instead of steam because of the ready availability of high pressure air at the tunnel site. Although the working gas is normally nitrogen or argon, other gases may be used. The first published description of this tunnel was that of Potter, et al. (Ref. 13).

2.2 INSTRUMENTATION AND CALIBRATION

Gas flow rate to the arc heater is measured through use of calibrated sonic-flow orifices, and reservoir pressure is measured with a Consolidated Electrodynamics Corporation Electromanometer®. Inaccuracy of these systems, on the basis of comparison with other means of measurement, and repeatability, are estimated to be less than ±0.5 percent for both flow rate and reservoir pressure.

Total enthalpy at the nozzle throat is determined by use of a calorimeter which, on the basis of comparison of results and repeatability, appears accurate to within ±4 percent limits of error. The measurement is supplemented by a probe system which measures local total enthalpy and mass flux in the test section with an estimated error limit of ±2 percent for mass flux and ±5 percent for enthalpy.

Impact pressures are measured with variable-reluctance, differential pressure transducers and water-cooled probes. Calibration of the transducers is accomplished by means of an oil-filled micromanometer and a McLeod gage. Inaccuracy in impact pressure measurement is believed not to exceed ±2 percent limits. Static pressures are measured by the same method but are not used for primary calibration purposes because of the very large corrections for viscous and rarefied flow phenomena.

The establishment of reservoir conditions, determination of impact pressures, and proof of inviscid, adiabatic core flow through the nozzles form part of the flow calibration. This information is used in a calculation which accounts for nonequilibrium expansion of the gas throughout the nozzle to yield the needed flow properties. Information on various aspects of these measurements is given by Potter, et al. (Ref. 14), Potter and Bailey (Ref. 15), Kinslow and Miller (Ref. 16), and Carden (Ref. 17).

Calibrations of the transducers were made at intervals during the test period, and the signal was continuously monitored on a strip chart to determine when equilibrium had been obtained. Run duration was typically several hours in length. Models were normally left in a low pressure environment for several days before data were obtained to complete the outgassing of the orifices and pressure lines.

The flow field was investigated using the impact pressure and hot-wire resistance anemometer probes as shown in Fig. 3. Both probes were operated in the axial and lateral directions by means of the tunnel probe carrier, which allowed an accuracy of better than 0.002 in. to be obtained in probe positioning. The impact pressure probe was water-cooled to a point 2 in. from the nose and was formed so that when the probe tip was positioned near the plate surface, the larger portion was effectively hidden downstream of the plate trailing edge. Linear growth of the impact and hot-wire probes, when exposed to the high temperature flow, was calibrated with an optical system which could monitor the probes throughout the test run.

2.3 NOZZLE FLOW CONDITIONS

Two separate contoured nozzles, having no radial or axial gradients in the test region, were used during the test. The stagnation conditions were such that the assumption of the flow being vibrationally frozen from the sonic point is justified. Flow field surveys in the test region are shown in Fig. 4 for each of the test flow conditions. General information on the undisturbed flow properties in the test region is given in Table I. A description of the design and calibration of the contoured aerodynamic nozzles will be given by Potter and Carden in a forthcoming AEDC report.

2.4 FLAT PLATE MODELS

A series of brass flat plates was constructed to enable a complete surface pressure distribution and flow field investigation to be conducted. Plates used for flow field surveys contained no pressure orifices. A schematic of the plate construction is shown in Fig. 3. The plate surface and leading edge were honed to obtain a smooth surface and a leading-edge radius of 4 to 6 x 10^{-4} in. Plate width was held constant at 1.5 in., which was approximately the isentropic core diameter of the nozzle flow. No pressure orifices were placed closer than 0.75 in. from the trailing edge, and no end effect on surface pressure distribution was found. Each plate was instrumentated with at least one internal thermocouple, and one plate was constructed with a series of thermocouples close to the surface to obtain a measurement of the surface temperature gradient. Leading-edge bevel angle was varied from 7.5 to 50 deg to study bevel angle effect, and various thicknesses of brass shim stock were cemented on selected plates to study the effect of leading edge thickness. Where pressure orifices very close to the leading edge were desired and the bevel angle was too small to place the pressure tube within the plate, small pressure tubes were cemented to the bottom surface close to, but not touching, the leading edge. Flow field surveys, with plates having these small external pressure tubes, indicated no influence on the external flow field. Orifice diameter varied from 0.030 to 0.100 in. A few orifices placed near the leading edge were drilled at an angle tangent to the lower surface bevel angle. This resulted in orifices of oval shape with the streamwise dimension being greater than the spanwise dimension. However, these orifices were on plates having bevel angles greater than 27.5 deg, and the data exhibited errors that were caused by the excessive bevel angle. This is discussed in greater detail in Section 3.1.2. The plates were carefully aligned in the tunnel test region using an optical system which insured consistent zero-angle-of-attack positioning. Also shown in Fig. 3 are the characteristic geometric parameters and sign notation used in the data presentation.

SECTION III
EXPERIMENTAL RESULTS

3.1 FLOW FIELD SURVEYS

Experimental studies of the boundary layer and shock structure above the surface of a sharp flat plate in the weak interaction regime are numerous. However, as the rarefaction level is increased, available experimental studies became meager. Investigations which concern shock and boundary-layer formation on cooled, sharp flat plates upstream of the

strong interaction regime include those of Nagamatsu, et al. (Ref. 18), Wallace and Burke (Ref. 19), and McCroskey, et al. (Ref. 20). The adiabatic wall case has been studied by Laurmann (Ref. 21), Chuan and Waiter (Ref. 22), and Rogers, et al. (Ref. 23). Schlieren photographs obtained by Nagamatsu, et al. (Ref. 18) were said to indicate reverse shock curvature near the leading edge. Also, the maximum shock angle was downstream of the leading edge rather than at x = 0. The first published boundary-layer surveys indicating fully merged flow on a cooled flat plate appear to be those of Wallace and Burke (Ref. 19). Impact pressure probe surveys obtained at values of $\bar{X}_{\infty, X}$ of 2 and 9 exhibited the classical, distinct, boundary-layer region, whereas for values of $\bar{X}_{\infty, X}$ = 47 and 85, the data appear to signify a fully merged shock and boundary layer. Shock wave slope, as determined from schlieren photographs, did not agree with strong interaction theory. However, the shock slope remained positive as the leading edge was approached. McCroskey, et al. (Ref. 20) have obtained measurements of shock wave and boundary-layer development substantially into the merged-layer regime. Measurements included schlieren and nitrogen flow discharge photographs, impact pressure probes, and hot-wire measurements. Various results of this investigation will be compared to the present data. Laurmann (Ref. 21), using a free-molecule probe, noted a delay in forming the boundary layer and shock wave for several mean free paths behind the leading edge. Chuan and Waiter (Ref. 22) used impact pressure surveys to deduce the shock layer position and velocity distribution through the boundary layer. Their results indicated a wedge-type flow with the shock originating from, or slightly ahead, of the plate leading edge. Very large slip velocities were inferred by extrapolating the impact pressure flow surveys to the plate surface. The low supersonic Mach numbers of the investigations of Rogers, et al. (Ref. 23) and Laurmann (Ref. 21) penetrated well into the strong interaction regime, with distinct regions of boundary layer and inviscid flow being identified by impact probe surveys.

In the present study, twenty discrete axial stations along the centerline of the plate were traversed in a direction normal to the plate by means of the impact and hot-wire probes. The interval in the normal direction, y, was one hundredth of an inch, and a complete survey was made during the continuous operation of the tunnel. Data were recorded instantaneously for the hot-wire measurements and required approximately three minutes for each impact probe measurement to reach equilibrium.

Since the data were obtained in the fully merged viscous layer regime, the determination of characteristic points of the flow field is difficult and to some extent must be considered arbitrary in nature. Figure 5 shows a typical flow survey through the shock layer and illustrates the difficulty of

identifying the boundaries of isentropic flow (y_A) or the "maximum slope" outer edge ($y_{\hat{A}}$). It is recognized that the peaks of the profiles (y_B) do not necessarily represent an exact border between the shock and the boundary layer. However, y_B represents a convenient reference quantity which can be determined accurately.

3.1.1 Corrections to the Measurements

The interpretation of pressure data obtained under conditions of high heat transfer requires corrections that are not ordinarily necessary. The necessity of employing an impact pressure probe of small dimensions to survey the viscous layer regime near the plate introduces viscous-induced errors in the measurements. This phenomenon, referred to herein as the viscous correction, has been studied extensively and reported in the literature. A recent study, under conditions applicable to the present work, has been reported by Potter and Bailey (Ref. 15). The effect of a temperature gradient along a small bore tube causing a pressure gradient to exist was first studied experimentally by Knudsen (Ref. 24) and more recently by Arney and Bailey (Ref. 25). This thermal transpiration correction can result in large errors under typical flow conditions in heated, low-density facilities. When orifices of small size are used to sense sufficiently low pressures, under conditions of high heat transfer, a form of nonequilibrium arising from unequal speed distributions between incoming and outgoing molecules in the orifice entrance region may cause considerable error in pressure measurement. This orifice effect recently has been studied by Potter, Kinslow, and Boylan (Ref. 26).

In order to determine the corrections necessary for quantitative study of measurements obtained by an impact pressure probe in the shock layer, a number of flow properties are required which are not known a priori. Although it was realized that exact corrections to the impact pressures to account for viscous, thermal transpiration, and orifice influences could not be made because of inadequate definition of the flow in the viscous shock layer, it was believed important to assess the approximate magnitude and trend of these corrections. Based on the following assumptions and procedures, the impact pressure data were corrected, and an example of the results is indicated in Fig. 6.

a. The shock in front of the impact pressure probe could be treated as a Rankine-Hugoniot normal shock.

b. The flow behind the oblique shock (region 1, Fig. 3) was computed from the experimental impact pressures and static wall pressures.

c. The static pressure distribution normal to the plate was assumed to be constant in the shock layer and to have a sine distribution through the shock.

d. The experimentally determined position of the shock was taken into account for the calculation of stagnation temperature.

e. The stagnation temperature was considered to decrease linearly to wall temperature.

f. Heat-transfer rate to the probe was based on the work of Potter and Miller (Ref. 27).

An examination of the data in Fig. 6 indicates a net change of about 10 percent at the maximum values of impact pressure, whereas near the surface of the plate the corrections tend to cancel. The corrections influence the determination of the maximum slope parameter, $y_{\acute{A}}$, but are negligible in determining the profile peak, y_B, and actual outer edge, y_A. All data obtained in flow field pressure surveys have been corrected for viscous, thermal transpiration, and orifice effects by the above approximate procedure.

3.1.2 Effect of Leading-Edge Wedge Angle and Thickness

Recent experimental investigations concerning the flow field and surface pressure distributions on sharp flat plates have been noted for their large discrepancies. Aside from the acknowledged difficulty of producing acceptable aerodynamic conditions and the instrumentation problems involved, the seemingly simple problem of producing a model which approaches the mathematical definition of "sharp" and "flat" has proven to be a source of difficulty. Instrumenting the surface of a flat plate, either with flush-mounted pressure transducers or pressure tubes to remote transducers, requires a plate of finite thickness. Plates with a lower surface bevel angle are therefore necessary if a very sharp leading edge is required. Based on continuum flow considerations, wedge angles on the order of 40 deg should be allowable, for the Mach number range generally involved in such investigations, before shock detachment appears. However, the large boundary-layer growth on the plate introduces a factor in the design of such models which can not easily be accounted for. In addition, the physical leading edge must be such as to approach the mathematically sharp leading edge of theoretical analyses. In the present case, leading-edge thicknesses of a fraction of a mean free path were obtained.

In order to experimentally study the effect of lower surface bevel angle and leading-edge thickness on the external flow field, a series of plates with varying bevel angles, as shown in Fig. 3, was constructed. Finite thicknesses of brass shim stock were attached to selected plates to study the effect of leading-edge thickness. A station 1 in. downstream of the leading edge was selected for surveying the effects on the flow field of

various bevel angles and leading edge thicknesses. Figure 7 indicates the results of this test. The distortion of the flow field, as compared between two different bevel angles, is seen in Fig. 7a. A complete shock peak survey is shown in Fig. 7b for varying bevel angle plates. It can be seen that for $\alpha \leq 27.5$ deg no distortion is apparent. Extrapolation of the data to the leading edge of the plate indicated that the shock had become detached or more thickened for the 40-deg bevel angle. This detachment was present even though the leading edge could be considered sharp, having a thickness of approximately 0.001 in. The effect of leading-edge bluntness is shown in Fig. 7c. Displacement of the shock away from the plate, with the addition of even small amounts of leading-edge bluntness, is apparent. However, this distortion appears to be very small as a leading-edge thickness of 0.001 in. is approached. This would seem to indicate that the requirement of a sharp leading edge has been approximated in the present case. The investigations of Hammitt, et al. (Ref. 28), Cheng, et al. (Ref. 29), and Harvey (Ref. 30) may be consulted concerning the relation between leading-edge bluntness effects and viscous interaction effects. Even when $Re_{\infty,t} = 11.5$ there are data (Ref. 30) which indicate a strong influence of leading-edge bluntness even in the viscous-dominated regime. In addition, Cheng, et al. (Ref. 29) noted the strong influence of freestream Reynolds number and wall temperature effects for a constant leading-edge bluntness. Hayes and Probstein (Ref. 1) have suggested the requirement that $Re_{\infty,t} << M_\infty^3$ before a strong interaction region is observable without marked effect of the blunt nose. Although the present results indicate that distortion of the shock layer is possible to values of $Re_{\infty,t}$ as low as unity, the influence on surface pressure or heat-transfer measurements remains to be seen. Where absolute determination of shock position is required, it appears necessary to have extremely sharp leading edges. The coupling of the bevel angle and leading-edge thickness influences are also indicated in Fig. 7c. The remainder of the flow field survey data presented herein is limited to those obtained using a flat plate having a bevel angle of 15 deg and leading-edge thickness of 0.001 in. or less.

3.1.3 Results and Discussion

The majority of the flow field surveys were obtained on the plate centerline. However, surveys 0.25 in. in either direction from the centerline were made to insure that the finite width of the plate was exerting no influence on the flow field. Measurements indicated essentially one-dimensional flow over this region.

Since various flat plate models contained water cooling systems which did not supply water closer than 0.75 in. to the leading edge, it was felt that an experimental determination of this temperature gradient along the

plate surface was necessary. A plate, having a relatively poor water cooling system, was instrumentated with five separate thermocouples at different chordwise locations buried slightly under the top surface and above the water passages. The plate was then tested at both flow conditions, and the results are shown in Fig. 8. Although a negative temperature gradient was found to exist from the leading edge downstream, the coldwall criterion was not violated. Values of T_w/T_o of approximately 0.1 and 0.2 are adequate to describe the conditions of the test.

Typical impact pressure and hot-wire surveys through the shock layer are indicated in Fig. 9. Values of the viscous interaction parameters, $\bar{v}_{\infty,x}$ and $\bar{\chi}_{\infty,x}$, are included in the figure. The fully merged characteristic of the flow, even at the trailing edge of the plate, can be seen. It is interesting to note that near the wall the profiles become increasingly divergent as the leading edge is approached. Very near the leading edge the determination of the characteristic points, as defined in Fig. 5, becomes rather arbitrary. Since the inlet diameter of the impact pressure probe is approximately fifty times larger than the hot-wire anemometer, the hot-wire measurements resulted in better definition of the flow near the leading edge.

A large number of profiles, as illustrated in Fig. 9, were analyzed to determine the shock layer over the length of the plate. Figure 10 indicates the characteristic point y_B and the shock angle θ. Indicated in the figure are several recent theoretical models. Near the leading edge, the present results would appear to contradict the results of Oguchi (Ref. 3) and Jain and Li (Ref. 6), but substantiate qualitatively the recent work of Pan and Probstein (Ref. 7). The flow model as proposed by Nagamatsu, et al. (Ref. 18), which predicts the delay of the shock formation for a distance $\zeta = M_\infty \lambda_\infty N$ and reverse curvature near the leading edge, is not supported by the present data. For the conditions of the present test, and a conservative value of 3.0 for the number of required collisions for zero slip, the parameter ζ would have a value of 1.22 in. The recent theoretical work of Chow (Ref. 9), who used a linear velocity profile and the Crocco integral relationship, agrees with the present results. The hot-wire measurements appear to give consistently lower values of y_B than the impact probe data. Measurements of wall pressure, obtained while traversing the flow with the impact pressure probe, indicated that a slight distortion of the flow field was likely when using this probe. It should also be noted that the data of Fig. 10 are based on the characteristic position y_B. Data interpretation using y_A or $y_{\acute{A}}$ would shift the data significantly. The large apparent thickness of the shock is indicated in Fig. 11. Because of this difficulty of data interpretation, comparison with theoretical results in Fig. 10 should be considered only from a qualitative point of view.

The slope of the shock wave was found to vary as the selection of the characteristic dimension was changed. For the range $0.39 \lesssim \bar{v}_{\infty,x} \lesssim 0.60$, the shock shape can be described as $y \sim x^n$, where the slope, determined experimentally, is given in the following table:

Characteristic Dimension	Impact Probe	Hot Wire
y_A	0.58 ± 0.04	0.44 ± 0.06
$y_{\acute{A}}$	0.62 ± 0.04	0.71 ± 0.07
y_B	0.80 ± 0.01	0.85 ± 0.05
y_{ms}	0.72 ± 0.04	0.73 ± 0.03

An example of the determination of the shock slope is shown in Fig. 11. For values of $\bar{v}_{\infty,x} \gtrsim 0.60$, shock curvature was apparent with the local shock angle increasing as the leading edge is approached (Fig. 10). Recently published data by McCroskey, et al. (Ref. 20) confirm that the "shock wave" represented by the profile peaks, y_B, exhibits a slope corresponding to $0.80 \lesssim n \lesssim 0.85$. The interaction of the impact pressure probe shock and the plate shock and surface, is believed to cause the differences in experimental shock slopes determined from hot-wire and impact probe measurements. Cheng, et al. (Ref. 29) predict that, in the region of strong interaction where bluntness effects are zero, the shock will have the form $y \sim x^{3/4}$.

The above discussion suggests the difficulty of data interpretation in the fully merged regime. Various theoretical models assume that either Hugoniot relations are valid for the shock or that the shock may still be considered thin as compared to the shock layer thickness. Continuity of mass flow between the freestream and the shock layer requires that the outer edge of the viscous shock layer lie at the center of the shock wave. The position of the shock center, however, is arbitrary (Ref. 7). If the characteristic dimension $y_{\acute{A}} - y_B$ is assumed to describe the shock thickness, Δ_{ms}, then the ratio of shock wave to shock layer thickness may be expressed as $\Delta_{ms}/y_{ms} = 2(y_{\acute{A}} - y_B)/(y_A + y_B)$. The present data, in terms of this parameter, are indicated in Fig. 12. Also indicated is the curve fit of the data presented by McCroskey, et al. (Ref. 20). The rarefaction level of $Re_{\infty,x}/M_\infty \approx 40$ to 45, suggested by Pan and Probstein (Ref. 7), at which the shock thickness should become important appears to be somewhat low.

Velocity distributions through the shock layer can be inferred from the measurements described above but must be considered qualitative in nature. An example of calculated velocity distributions for four axial stations is shown in Fig. 13a. Assumptions regarding these calculations

were identical to the probe viscous correction calculations. An inspection of the profiles indicates that a linear velocity distribution is not unreasonable. The slip velocity at the wall can be approximated by extrapolation of these profiles to y = 0 and is indicated in Fig. 13b.

For estimating slip velocity, another technique was suggested* which avoids assuming any flow properties normal to the plate and does not require the tedious calculation of the velocity distributions. From considerations of continuity and momentum, one may write

$$u_w = \left\{ p_{2,\,o,\,w} \Big/ \left[\rho_w \left(1 - \epsilon_w/2 + p_w/\rho_w u_w^2 \right) \right] \right\}^{1/2}$$

This procedure requires an extrapolation of the measured values of $p_{2,0}$ to y = 0; the density at the wall was calculated from measured surface temperature and pressure. The result of this calculation is also indicated in Fig. 13b. Agreement with the result obtained using the extrapolated velocity distributions is good except near the leading edge. Even though this latter technique avoids several assumptions used in calculating the velocity distributions, the calculation is strongly dependent on measured impact pressures in a region where some flow field distortion caused by the presence of the probe may have occurred, and viscous and rarefied flow influences on the probe were present. However, the qualitative trend of the data is quite reasonable. The theoretical results of Chow (Ref. 9) and Oguchi (Ref. 2) are indicated in the figure. The present data suggest that slip could be expected to extend well into the strong interaction regime. This was predicted by the theoretical results of Pan and Probstein (Ref. 7), but their predicted decrease of the slip velocity near the leading edge is not seen. The slip velocity, as shown in Fig. 13, should approach zero as $\bar{v}_{\infty,\,x}$ approaches zero, and failure of the data to clearly indicate this trend at the lower values of $\bar{v}_{\infty,\,x}$ is evident. However, a linear curve fit through the data at the higher values of $\bar{v}_{\infty,\,x}$, for the method using extrapolated impact pressures, appears reasonable.

Apparent shock strength indicated by peak values of $p_{2,\,o}/p_{\infty,\,o}$ (read at y_B) are shown in Fig. 14. Obviously, because the shock layer was fully merged, what is called "apparent shock strength," here really should not be confused with the customary definition of shock strength, i.e., the present shock did not correspond to the classic Rankine-Hugoniot Shock in an inviscid flow field.

3.2 SURFACE PRESSURE MEASUREMENTS

Experimental measurements of surface pressure and heat-transfer distributions are more numerous than studies of shock layer formation

*Suggested by J. L. Potter, Manager, Aerophysics Branch, VKF.

and structure. However, in regard to the measurement of surface pressure distribution, the situation has become extremely confused because of the wide disagreement between various investigations. Surface heat-transfer distribution appears to be better established, both theoretically and experimentally, from the strong interaction regime to the near-free-molecular flow limit. The present discussion is limited to the region near the leading edge where large departures from strong interaction theories have been noted. It is in this region that correlation of data from different facilities has been largely unsuccessful.

The hypersonic shock tunnel experiment of Nagamatsu, et al. (Ref. 18) appears to be the first which extended data upstream of the strong interaction regime. The results not only indicate large departures from the extrapolation of strong interaction theory, but suggest the existence of a pressure peak as the leading edge is approached. The terms pressure peak and pressure plateau are used herein to signify a pressure gradient reversal occurring over a short chordwise length as opposed to a near constant pressure level with a smaller gradient over a comparatively longer chordwise length. Further shock tunnel experiments were performed by Vidal and Wittliff (Ref. 31). These data confirm qualitatively the data of Nagamatsu, et al. However, some of their results are for a considerably lower pressure level and exhibit an extensive plateau region. Discussions of these data by Vidal and Bartz (Ref. 32) and Garvine (Ref. 8) indicate that the normal stress effects described herein as the "orifice effect" cause the data to be somewhat in error, and the plateau indication may have been false. The investigation of Vas, et al. (Ref. 33), which utilized a continuous, heated nitrogen tunnel, also indicated large departures from strong interaction theory.

The viscous interaction parameter, $\bar{v}_{\infty, x}$, suggested by Talbot (Ref. 5), was first employed in the present problem by Deskins (Ref. 34). Data obtained in a "hotshot" facility, as well as from the tunnel employed by the present authors, confirmed that initial departures from strong interaction theory corresponded to $\bar{v}_{\infty, x} \approx 0.1 - 0.2$. The recent report of Moulic (Ref. 35) includes a comprehensive discussion of adiabatic-wall data. Available experimental cold-wall data, upstream of the strong interaction regime, are summarized in Table II.

As previously mentioned, the present surface pressure measurements required a relatively long run duration in order to achieve equilibrium. The normal operation of the tunnel required two or three days before a single plate, having one to four pressure orifices, was surveyed. Also, the tunnel was kept at a low pressure level for several days before testing to aid in outgassing. Figure 15 indicates a typical data acquisition for a single orifice. The observed effect of an initial pressure rise and slow decrease is probably a combination of tube outgassing and pressure lag.

3.2.1 Correction to the Measurements

Of the three pressure corrections discussed in conjunction with the shock layer, impact-pressure measurements, only the influence of the heat transfer to the pressure orifice region is applicable to the surface pressure measurements. However, under the conditions of the present test, this correction is quite large and would cause a serious misinterpretation of the data if not taken into account. Semiempirical curves of Potter, et al. (Ref. 26) allow this correction to be applied to the measured pressures. Since the local heat-transfer rate is required for this correction, and the present investigation did not include such measurements, experimental results from various sources have been used in the present case. Figure 16 shows a typical set of results and the data as corrected for the orifice effect. The remaining data plots, unless noted, show data which have been corrected for this effect.

3.2.2 Effect of Leading-Edge Wedge Angle

Several plates having lower surface wedge angles of 15, 27.5, 40, and 50 deg were tested, and the results are indicated in Fig. 17. The conclusion obtained from the shock layer surveys indicating shock distortion at the higher wedge angles is confirmed by these data. Surface pressure measurements to show the effect of varying leading-edge thickness were not made. Data obtained on plates having wedge angles greater than 27.5 deg are omitted from subsequent correlations.

3.2.3 Results and Discussion

A series of ten individual flat plates, each containing from one to four orifices, enabled a streamwise pressure distribution from x = 0.026 to 4.00 in. to be made. For the lower wedge angles, the orifice closest to the leading edge was at x = 0.048 in.

The present results are shown in Fig. 18 correlated as the ratio of surface-to-free-stream pressure versus the strong interaction parameter, $\bar{\chi}_{\infty, x}$. Also indicated is the strong interaction theoretical result of Cheng (Ref. 29) and a summary of typical experimental results from previous investigations. The poor correlation with the strong interaction parameter has been noted by various investigators.

Defining the relevant parameter as the ratio λ_1/δ^*, where λ_1 is evaluated downstream of the leading-edge shock, Talbot (Ref. 5) predicted that departures from strong interaction theory should be correlated by the viscous interaction parameter, $\bar{v}_{\infty, x}$. Also, to the first order, $\lambda_1/\delta^* = f(\gamma)\ (\bar{v}_{\infty, x})^2$. A correlation using the pressure coefficient, C_p, and viscous interaction parameter, $\bar{v}_{\infty, x}$, was performed, and the results

are indicated in Fig. 19. The small differences in wall temperatures between various sets of data could cause the variations in C_p. Also, a value of $\gamma = 1.4$ was assumed for the data correlation, which may not be entirely valid for all cases. Strong interaction theory appears to fail in the range $0.1 \lesssim \bar{v}_{\infty, x} \lesssim 0.3$, as suggested by Talbot (Ref. 5). To the zeroth order, strong interaction theory results in a relationship of the form*

$$p_w/p_\infty = C\bar{X}_{\infty, x}$$

When converted to C_p and $\bar{v}_{\infty, x}$, a relationship of the form

$$C_p = 2/\gamma C\ \bar{v}_{\infty, x} - 2/\gamma M_\infty^2$$

results. For large values of M_∞, the second term may be neglected. However, to illustrate the magnitude of this term, it has been retained in the present case and the strong interaction theory of Cheng (Ref. 29) is indicated in Fig. 19 for $M_\infty = 10$ and 20. The strong influence of Mach number on the initial departure from strong interaction theory, in terms of $X_{\infty, x}$, can be seen by setting $\bar{v}_{\infty, x} \approx 0.15$, as indicated in Fig. 19, and noting that when $\bar{v}_{\infty, x} \approx 0.15$ and $\bar{X}_{\infty, x} \approx \bar{v}_{\infty, x} M_\infty^2$, the initial departure of Mach 10 data should occur at $\bar{X}_{\infty, x} \approx 15$, and Mach 25 data would depart at $\bar{X}_{\infty, x} \approx 94$. An inspection of Fig. 18 confirms these results qualitatively. Following from this, it is apparent that, if the criterion for strong interaction is $\bar{X}_{\infty, x} \gtrsim 10$, then strong interaction will not exist unless $M_\infty \gtrsim 8$.

The free-molecular flow limit for a typical flow condition and diffuse reflection is also indicated in Fig. 19. The expected pressure drop to the leading-edge value is not seen. The data suggest at least a local pressure plateau extending to an undetermined value of $\bar{v}_{\infty, x}$ greater than the present experimental limit.

The strong influence of wall temperature on the absolute pressure level is indicated in Fig. 20. The adiabatic-wall data of Moulic (Ref. 35) and data obtained by the present authors are included for comparison. Also emphasized is the extensive axial length, in terms of $\bar{v}_{\infty, x}$, of the pressure plateau. The adiabatic-wall and cold-wall results indicated in this figure appear to be the most conclusive experimental determination of the existence of the pressure plateau. It should be noted that Moulic interpreted his data as a pressure peak with subsequent dropoff toward the free-molecular flow limit. The present data could also be interpreted in this manner, but the pressure gradient is not well defined and the term "local plateau" appears to be more descriptive.

---

*Except for an insulated plate, calculations beyond the zeroth order have not been done to the author's knowledge.

3.2.4 Comparison with Theory in the Merged-Layer Regime

Several quantitative predictions of the behavior of the pressure distribution in the merged-layer regime are available in the literature. Some of these results are compared to the present experimental data in Fig. 21. The data (in this figure) are limited only to those having a wall-to-stagnation temperature of approximately 0.10 since various theoretical results are for this value. Several comments concerning these theoretical predictions, as compared to the present data, are warranted. As shown in Figs. 18 and 19, strong-interaction theory fails in the merged-layer regime, and it has been shown in Fig. 21 only for comparative purposes. Pan and Probstein (Ref. 7) produced numerical calculations which, through correlation formulas, may be directly compared to the present results. Quantitative comparison with the experimental results is not good for $Re_{\infty, x}/M_{\infty} \lesssim 100$, but it is excellent above that limit, as shown in Fig. 22.

Since the free-molecular flow limit for a flat plate at zero incidence with completely diffuse reflection is expressed as

$$(p_w/p_\infty)_{FM} = 1/2 \left[1 + (T_w/T_\infty)^{1/2}\right]$$

the effect of Mach number would be indicated only through its effect on the ratio of wall-to-freestream temperatures. From practical considerations, this limiting value of p_w/p_∞ would not vary more than $1.2 \lesssim p_w/p_\infty \lesssim 2.0$ for cooled plates in current test facilities producing the required flow for near-free-molecular investigations. Since the parameter $M_\infty/Re_{\infty, x}$ is proportional to the Knudsen number, the method of correlation used in Fig. 22 would appear to be adequate if measurements very near to the free-molecular flow regime were made. The present correlation, using the viscous interaction parameter, $\bar{v}_{\infty, x}$, and pressure coefficient, C_p, could be expected to fail very near the leading edge for data representing wide variations in freestream Mach number. This follows from noting that the free-molecular flow limit, in terms of C_p, is expressed as

$$(C_p)_{FM} = \left\{1/2 \left[1 + (T_w/T_\infty)^{1/2}\right] - 1\right\} 2/\gamma M_\infty^2$$

Thus, in a region of free-molecular flow, a strong Mach number influence on the C_p could be expected.

The fully viscous, shock layer analysis of Oguchi (Ref. 3), with wall slip and thin shock wave assumptions, results in the pressure distribution shown in Fig. 21 as curve C. The hypersonic approximations,

$$p_w/p_\infty = \left[2\gamma/(\gamma + 1)M_\infty^2\right]\theta_S^2$$

and

$$\sin^2 \theta_S = \theta_S^2$$

used by Oguchi limits his results to Mach numbers much greater than unity. This is a common assumption used by various authors and introduces an error which is not negligible when compared to data obtained at Mach numbers comparable to the present results. However, the quantitative comparison in Fig. 21 would not be improved by the use of the exact relationships. The steep negative pressure gradient upstream of the plateau, caused by the theoretical shock curvature, is not seen in the present data. Oguchi's model, excluding slip, has been treated by Jain and Li (Ref. 6), and a typical result is shown in Fig. 21. A serious problem concerning the regime of validity is involved in these results. They used the experimentally determined maximum pressure found by Nagamatsu as the point x = 0. This would indicate that curve D in Fig. 21 must be shifted downstream an undeterminable amount. The slope of the theoretical results does not appear unreasonable, but a quantitative comparison is not possible because of this difficulty. Moulic (Ref. 35) also commented on this problem.

A linear velocity distribution was assumed by Chow (Ref. 9) who also accounted for the finite wave thickness. His results for a Mach number of 10 and T_W/T_O of 0.1 are indicated as curve E in Fig. 21. Although the theoretical results fail at a value of $\bar{v}_{\infty,X}$ of about 0.4, this was expected because kinetic flow concepts were not included in the basic analysis. Chow stipulated the necessity of matching his solution to first-collision theory.

The first-collision analysis of Charwat (Ref. 10) predicts the existence of a pressure plateau at a specific distance downstream of the leading edge corresponding to the edge of the initial collision regime. This plateau is continued downstream until a sufficient number of collisions occur to establish a continuum flow. The actual numerical calculation of the expected pressure plateau value involves proportionality constants which must be determined from experimental results. At the time Charwat formulated his theory, the data of Nagamatsu, et al. (Ref. 18) were the only available data to use for estimation of the pressure peak. Using these data and assuming fully diffuse reflection, Charwat arrived at values of C = 0.33 and D = 25 as being the most reasonable for the required empirical constants. When these values are applied to the present data, the theory for the higher wall temperature ratio agrees quite well with the data but theory and data disagree at lower wall temperature ratio. Since Charwat's analysis should become more accurate as wall temperature is reduced, this result indicated that an improvement to the empirical constants could be obtained. Using the two sets of data of the present investigation, the constants were reformulated, and values of C = 0.33 and D = 10 were obtained. Using these values, the theory of Charwat is shown in Fig. 21 for a Mach number of 10.15 and T_W/T_O of 0.1. Both the magnitude and

length of pressure plateau, as predicted by Charwat, are indicated in the figure. The effect of Mach number on the pressure peak, in terms of the pressure coefficient, C_p, is indicated in Fig. 23. Estimated maximum values of several of the experimental investigations summarized in Figs. 18 and 19 are included in the figure. Although the data are of such nature as to discourage comparisons of this sort, the results indicate that the empirical constants, as determined in the present study, offer an improvement over the original estimates of Charwat. Additional experimental studies, at varying Mach numbers, would no doubt provide improved estimates.

Returning to Fig. 21, it should be noted that the cold-wall ($T_w = T_\infty$), near-free-molecular flow results of Bird (Ref. 12) are included even though the calculations were performed at a speed ratio, S_∞, less than the conditions of the present test. Even for Knudsen numbers as large as ten, Bird predicted that the pressure will not have decreased to the free-molecular flow value. However, a negative pressure gradient is predicted which is not evident in the present data. The near-free-molecular theory of Kogan (Ref. 11), while providing numerical results, is not near the flow conditions of the present test and therefore can not be directly compared. The theoretical result of Bird (Ref. 12) indicates the total absence of a region of free-molecular flow attributable to collisions at the leading edge between incident molecules and the molecules reflected from the downstream portion of the plate. The difficulty of confirming this experimentally can be realized by noting that a pressure point 0.004 in. from the leading edge would be required for a Knudsen number of ten to be achieved at the most rarefied flow condition of the present test.

SECTION IV
CONCLUDING REMARKS

One apparent anomaly is suggested when comparing the present flow field surveys to the wall pressure distribution measurements. The shock angles in Fig. 10 indicate that, for Rankine-Hugoniot conditions, the pressure should continue to rise as the leading edge is approached, provided that pressure is invariant with y. This is contradicted by the present surface measurements which are constant near the leading edge. However, the flow near the leading edge is far removed from Rankine-Hugoniot, shock layer structure. The wedge-type flow with surface slip proposed by Oguchi (Ref. 3), or the theory of Charwat (Ref. 10), furnishes a physical explanation of the observed pressure plateau.

Extrapolation of the present shock survey measurements to the vicinity of the leading edge fails to confirm the delayed formation of the shock wave and boundary layer suggested by several previous investigations. Either a shock-weakening phenomenon or slip extending into the strong-interaction regime may be inferred from the present measurements (cf. the theory of Pan and Probstein, Ref. 7). McCroskey, et al. (Ref. 20), observed large reductions in the density ratio, ρ_1/ρ_∞, in the merged regime as the leading edge was approached. This implied reduced pressure immediately behind the shock even though the shock angle was increasing. The present results substantiate this conclusion and may indicate the the shock structure is the dominate mechanism upstream of the strong interaction regime.

Although measurements corresponding to a Knudsen number on the order of unity were obtained, the surface pressure measurements indicated no substantial trend approaching the free-molecular flow limit. The recent theoretical results of Kogan (Ref. 11) and Bird (Ref. 12) indicate that such an experimental result is not unreasonable. The present investigation indicates that the onset of merging corresponds to initial departures of p_w/p_∞ or C_p from strong interaction theory, whereas the pressure plateau signifies entrance into the transition regime. These occur at $\bar{v}_{\infty,x} \simeq 0.15$ and 0.6, respectively. It appears that the thickness of the shock wave is much greater than assumed in available theoretical flow models.

REFERENCES

1. Hayes, Wallace D. and Probstein, Ronald F. Hypersonic Flow Theory. Academic Press, 1959, p. 368.
2. Oguchi, H. Rarefied Gas Dynamics. Supplement 1, 1961, p. 501.
3. Oguchi, H. Rarefied Gas Dynamics. Supplement 2, Vol. II, 1963, p. 181.
4. Laurmann, J. A. "Hypersonic Interaction at High Altitudes." Lockheed Missiles and Space Co. R-6-90-63-83, Gas Dynamics RR 8-63-13, September 1963.
5. Talbot, L. "Criterion for Slip near the Leading Edge of a Flat Plate in Hypersonic Flow." AIAA Journal, Vol. 1, No. 5 May 1963, pp. 1169-1171.
6. Jain, A. C. and Li, T. Y. "A Critical Assessment of the Problem of Sharp Leading Edge of a Flat Plate in Hypersonic Flow." University of Cincinnati TR-AE-6401 (AD 608294), July 1964.

7. Pan, Y. S. and Probstein, R. F. "Rarefied Flow Transition at a Leading Edge." M.I.T. Fluid Mechanics Laboratory Pub. No. 64-8, 1964.

8. Garvine, Richard W. "On Hypersonic Flow Near a Sharp Leading Edge." Princeton University Report 755, 1965.

9. Chow, W. L. Private Communication (submitted to AIAA J.) 1966.

10. Charwat, A. F. Rarefied Gas Dynamics. Supplement 1, Vol. I, 1961, p. 553.

11. Kogan, M. N. "On the Computation of Flow at Large Knudsen Numbers." Astronautica Acta, Vol. 11, No. 1, Jan.-Feb. 1965, pp. 36-42.

12. Bird, G. A. "Aerodynamic Properties of Some Simple Bodies in the Hypersonic Transition Regime." AIAA Journal, Vol. 4, No. 1, January 1966, pp. 55-60.

13. Potter, J. L., Kinslow, M., Arney, G. D., Jr., and Bailey, A. B. Progress in Astronautics and Rocketry. Academic Press, New York, 1962, pp. 599-624.

14. Potter, J. L,, Arney, G. D., Jr. Carden, W. H., and Kinslow, Max. Proceedings of AGARD Fluid Dynamics Panel Specialists' Meeting, Arc Heaters and MHD Accelerators for Aerodynamic Purposes, AGARDograph 84, 1964, pp. 379-412.

15. Potter, J. L. and Bailey, A. B. "Pressures in the Stagnation Regions of Blunt Bodies in Rarefied Flow." AIAA Journal, Vol. 2, No. 4, April 1964, pp. 743-745.

16. Kinslow, Max and Miller, J. T. "The Nonequilibrium Expansion of a Diatomic Gas through a Convergent-Divergent Nozzle." AEDC-TR-65-103 (AD464533), June 1965.

17. Carden, W. H. "Experimental Heat Transfer to Hemispheres in Nonequilibrium Dissociated Hypersonic Flow with Surface Catalysis and Second-Order Effects." AIAA Third Aerospace Sciences Meeting, AIAA Preprint No. 66-3, January 1966.

18. Nagamatsu, H. T., Sheer, R. E., Jr., and Schmid, J. R. "High Temperature Rarefied Hypersonic Flow over Flat Plate." ARS Journal, Vol. 31, No. 7, July 1961, pp. 902-910.

19. Wallace, J. E. and Burke, A. F. Rarefied Gas Dynamics. Supplement 3, Vol. I, 1965, p. 487.

20. McCroskey, W. J., Bogdonoff, S. M., and McDougall, J. G. "An Experimental Model for the Leading Edge of a Sharp Flat Plate in Rarefied Hypersonic Flow." AIAA Third Aerospace Sciences Meeting, AIAA Preprint No. 66-31, January 1966.

21. Laurmann, J. A. "The Free Molecule Probe and Its Use for the Study of Leading Edge Flows." Physics of Fluids, Vol. 1, No. 6, Nov.-Dec. 1958, pp. 469-477.

22. Chuan, R. L. and Waiter, S. A. Rarefied Gas Dynamics. Supplement 2, Vol. II, 1963, p. 328.

23. Rogers, E. W. E., Berry, C. J., and Davis, B. M. "An Experimental Investigation of the Interaction between a Forward-Facing Step and a Laminar Boundary Layer in Supersonic, Low-Density Flow." National Physical Lab., Teddington, England, NPL-AERO-1139, ARC 26,656, FM-3563, X66-10942, January 1965.

24. Knudsen, Martin. Annalen der Physik, Vol. 31, 1910, pp. 205-229.

25. Arney, G. D., Jr. and Bailey, A. B. "Effect of Temperature on Pressure Measurements." AIAA Journal, Vol. 1, No. 12, December 1963, pp. 2863-2864.

26. Potter, J. L., Kinslow, M., and Boylan, D. E. Rarefied Gas Dynamics. Supplement 3, Vol. II, 1965.

27. Potter, J. L. and Miller, John. "Total Heating Load on Blunt Axisymmetric Bodies in Low-Density Flow." AIAA Journal, Vol. 1, No. 2, February 1963, pp. 480-481.

28. Hammitt, A. G., Vas, I. E., and Bogdonoff, S. M. "Leading Edge Effects on the Flow over a Flat Plate at Hypersonic Speeds." Princeton University R-326 (AD74339), September 1955.

29. Cheng, H. K., Hall, J. G., Golian, T. C., and Hertzberg, A. "Boundary-Layer Displacement and Leading-Edge Bluntness Effects in High-Temperature Hypersonic Flow." J. Aero. Sci., Vol. 28, No. 5, May 1961, pp. 353-81.

30. Harvey, W. D. "Effects of Leading-Edge Bluntness on Pressure and Heat Transfer Measurements over a Flat Plate at a Mach Number of 20." NASA TN D-2846, October 1965.

31. Vidal, R. J. and Wittliff, C. E. Rarefied Gas Dynamics. Supplement 2, Vol. II, 1963, p. 343.

32. Vidal, R. J. and Bartz, J. A. Rarefied Gas Dynamics. Supplement 3, Vol. I, 1965, p. 467.

33. Vas, I. E., McDougall, J., Koppenwallner, G., and Bogdonoff, S. M. Rarefied Gas Dynamics. Supplement 3, Vol. I, 1965, p. 508.

34. Deskins, H. W. "Correlation of Flat-Plate Pressures Using the Rarefaction Parameter $M_\infty C_\infty^{1/2}/Re_{x_\infty}^{1/2}$." AIAA Journal, Vol. 2, No. 3, 1964, pp. 573-574.

35. Moulic, E. S., Jr. NSF Grant NSF GP-2520 Series 7, Issue No. 3, 1966.

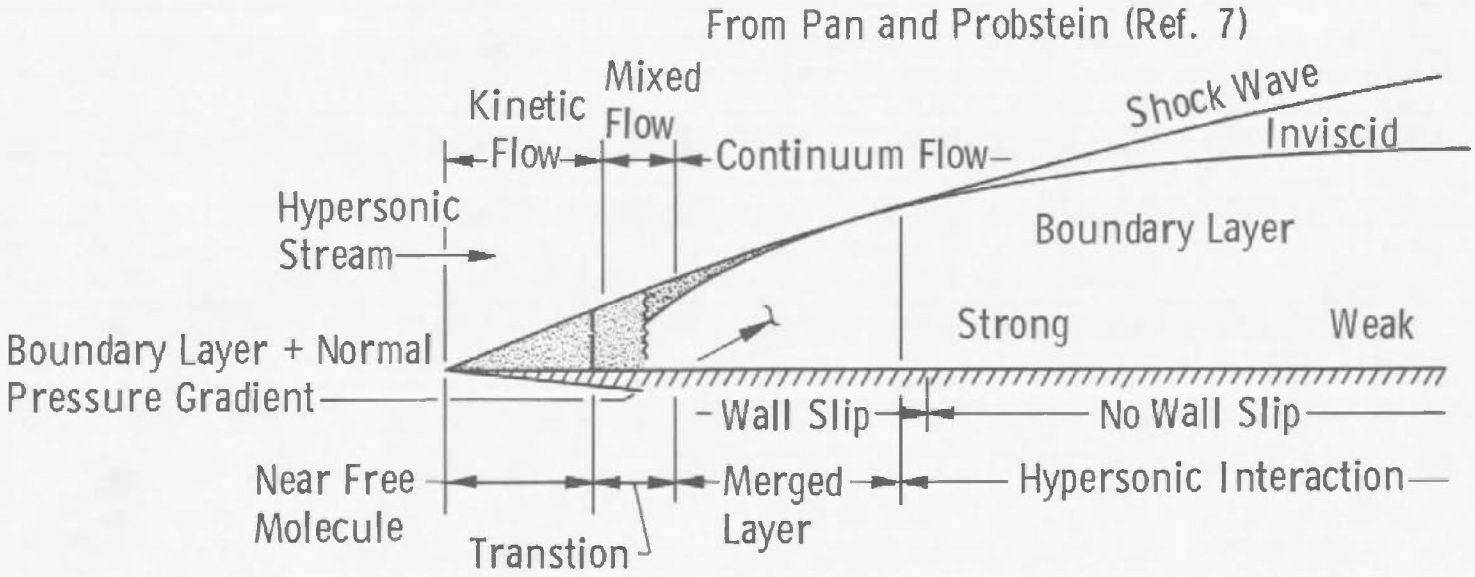

Fig. 1 Hypersonic Rarefied Flow Past a Semi-Infinite Sharp-Leading-Edge Flat Plate

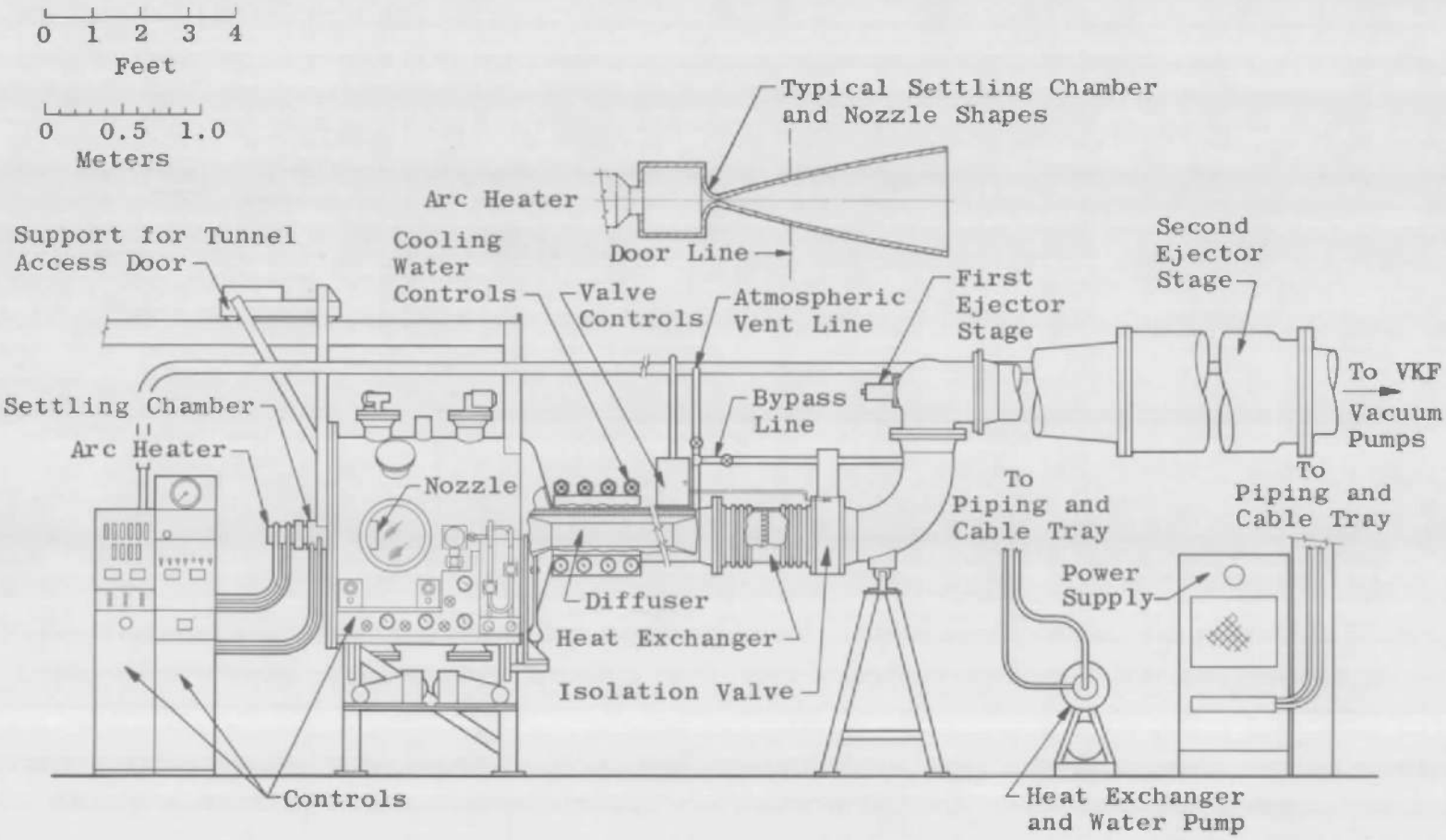

Fig. 2 Elevation View of Tunnel L

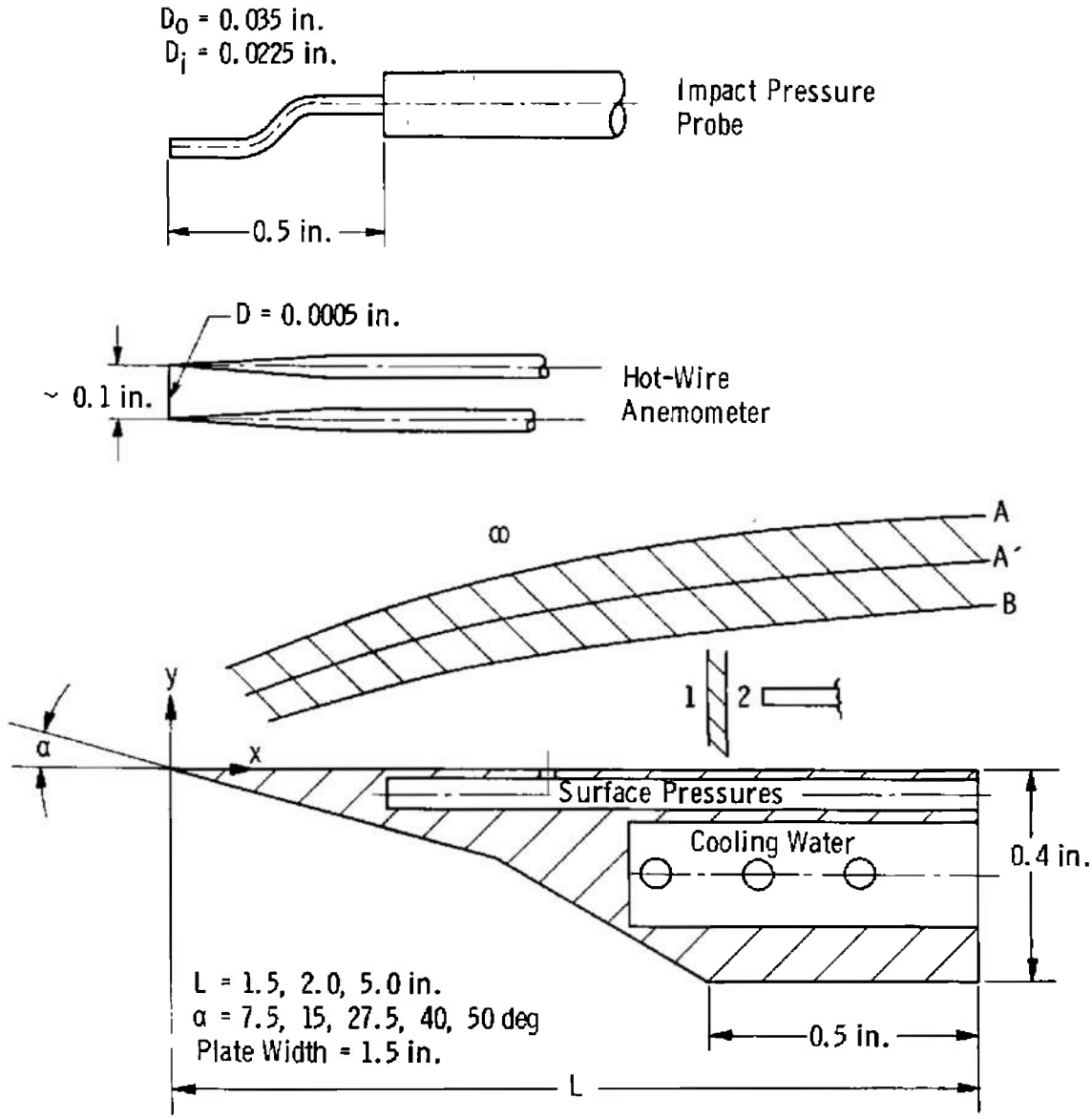

Fig. 3 Plates, Probes, and Flow Field Nomenclature

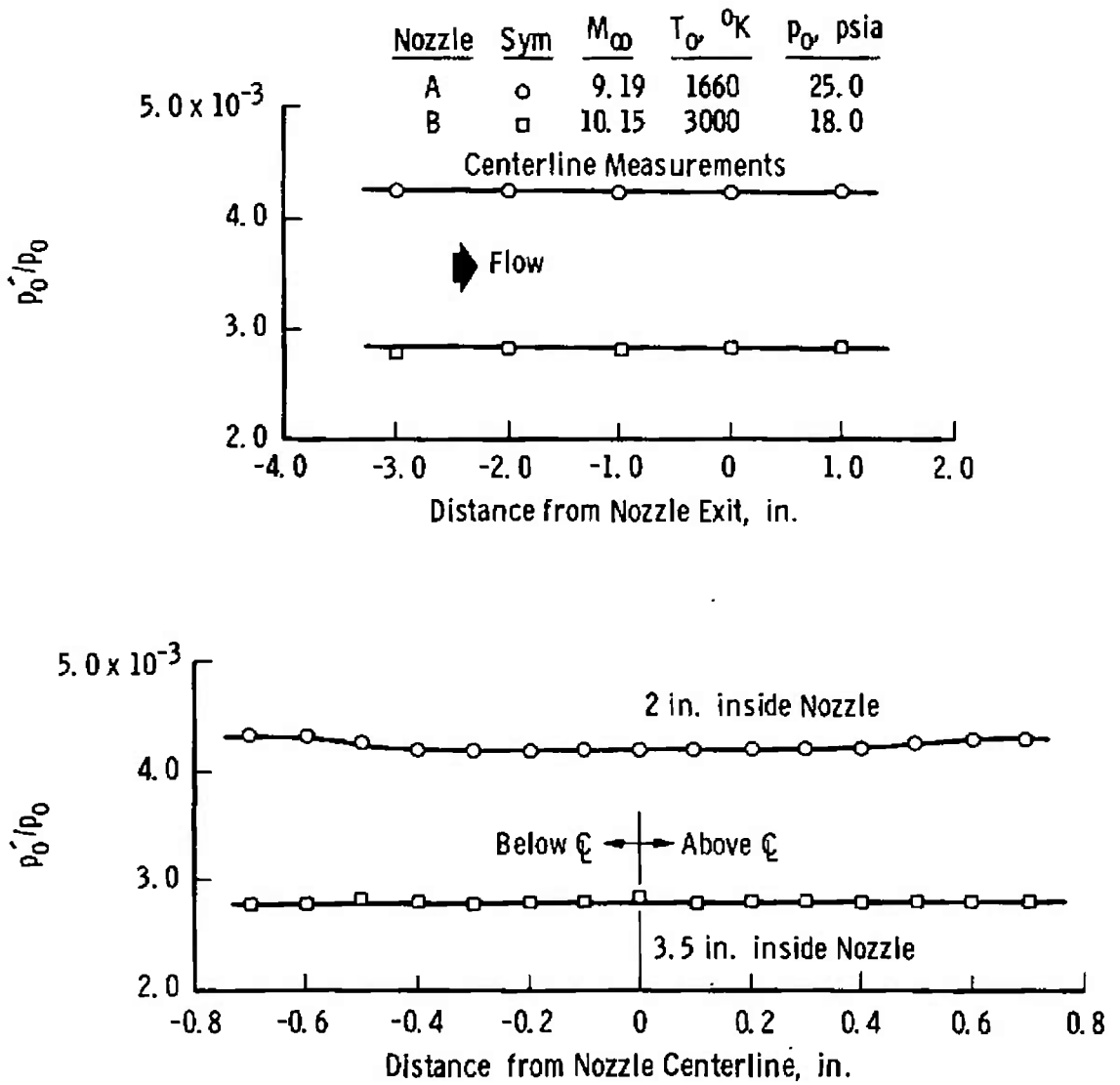

Fig. 4 Lateral and Transverse Flow Surveys

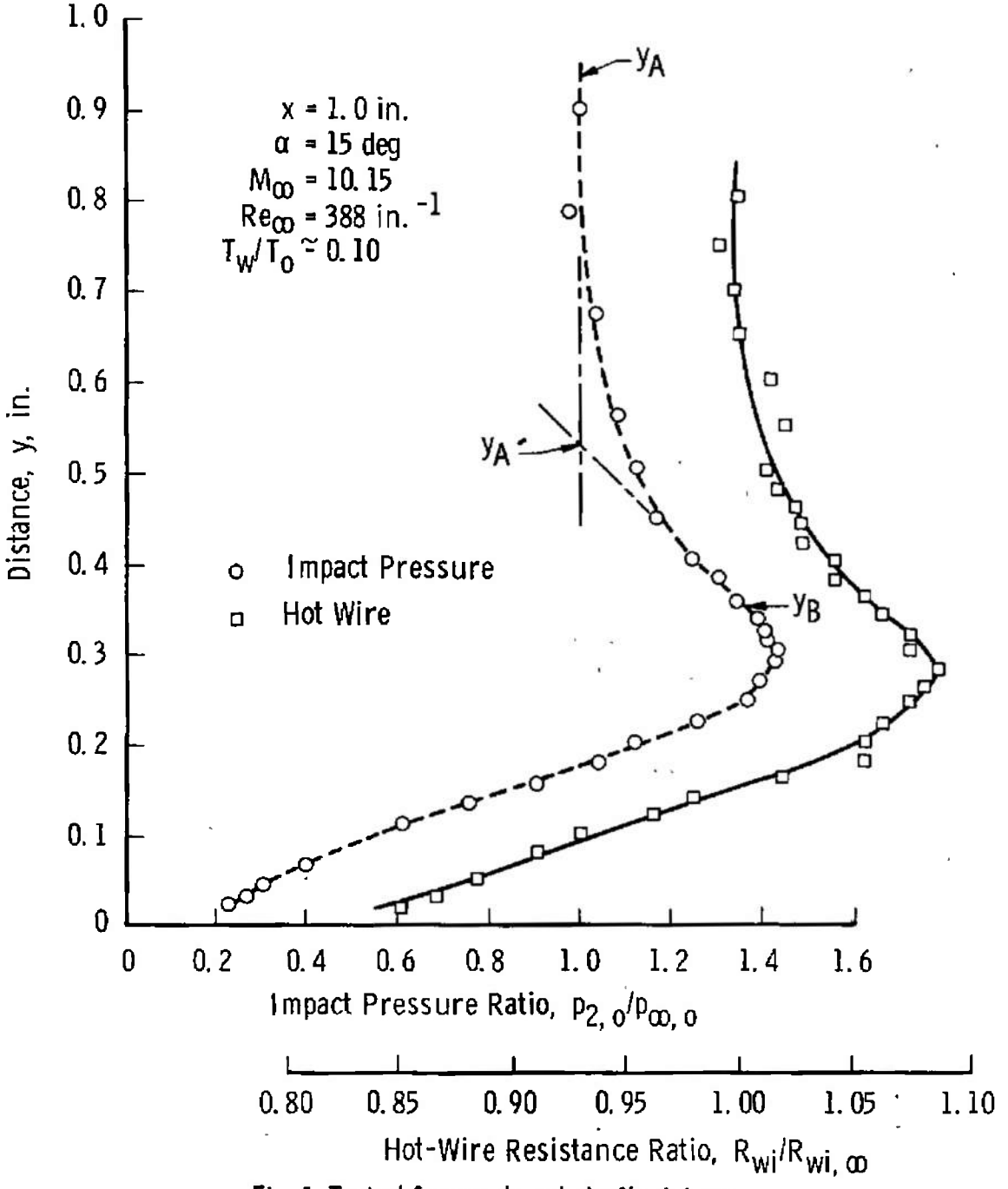

Fig. 5 Typical Surveys through the Shock Layer

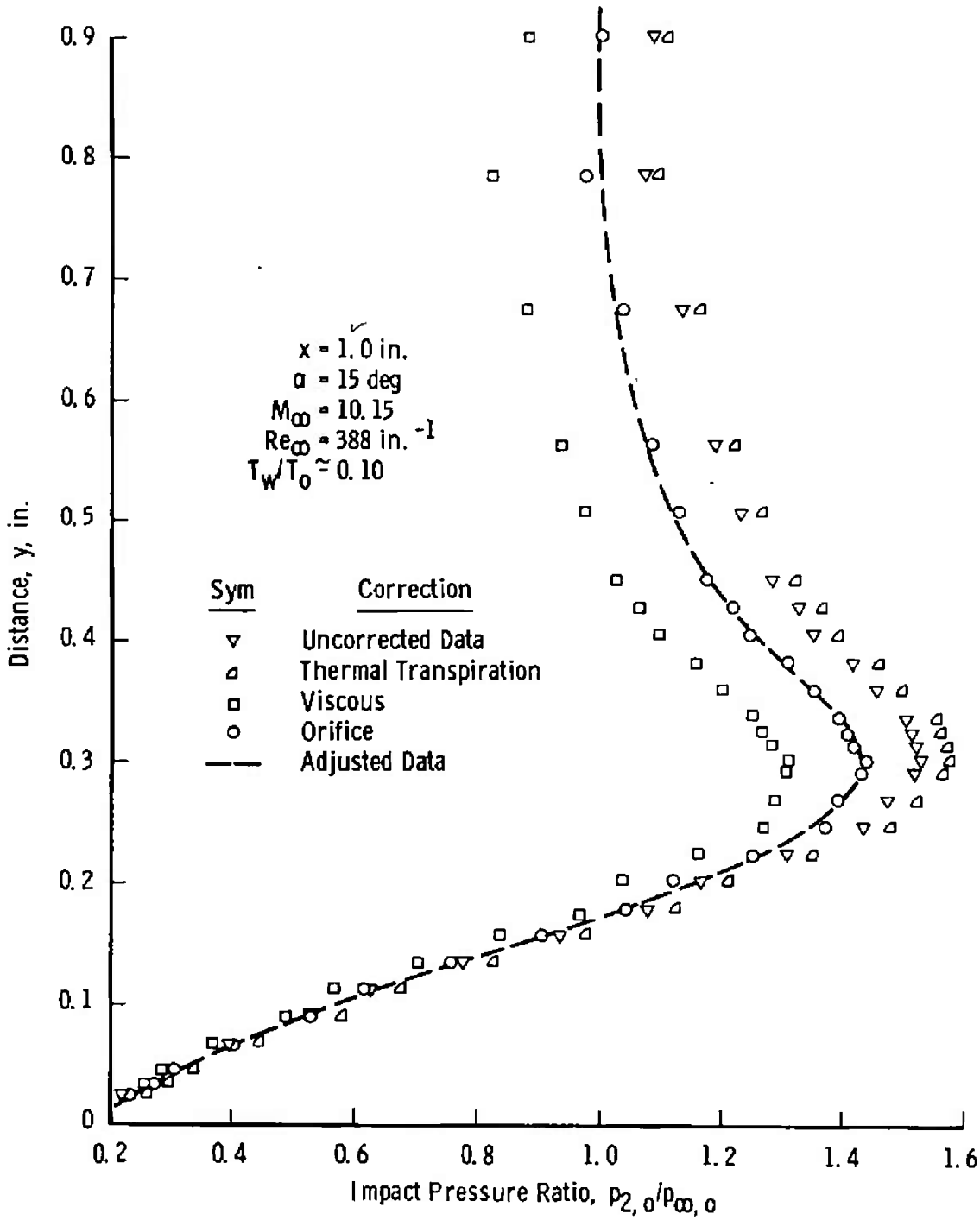

Fig. 6 Influence of Impact Pressure Corrections

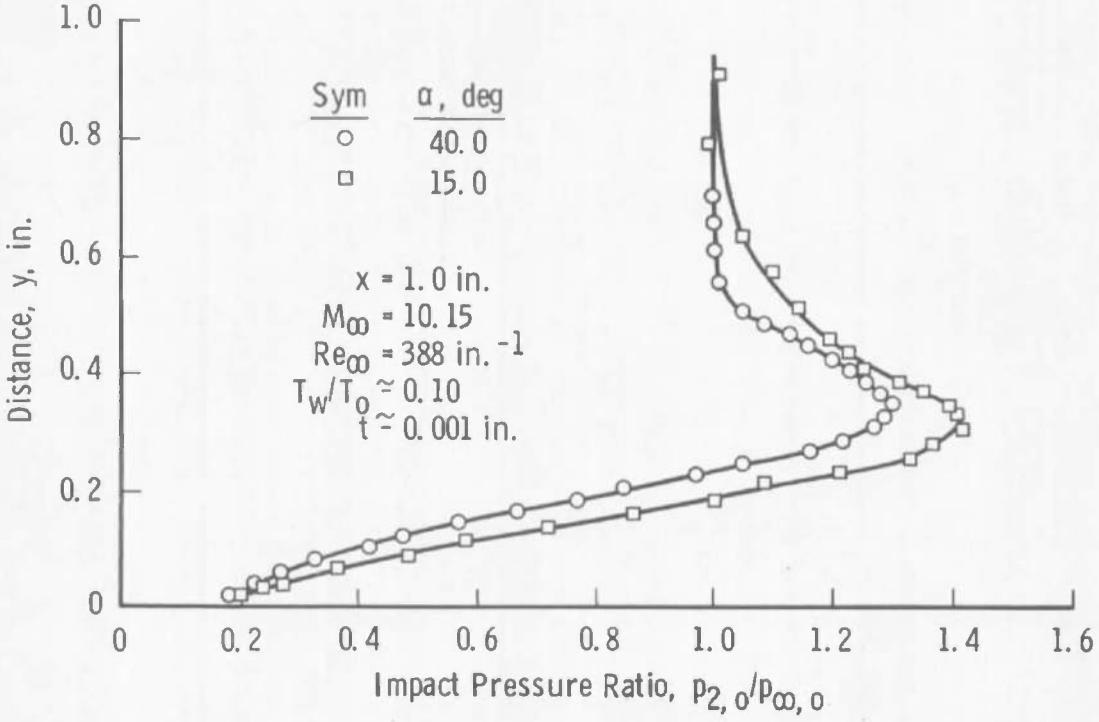

a. Flow Distortion in Shock Layer Caused by Plate Bevel Angle

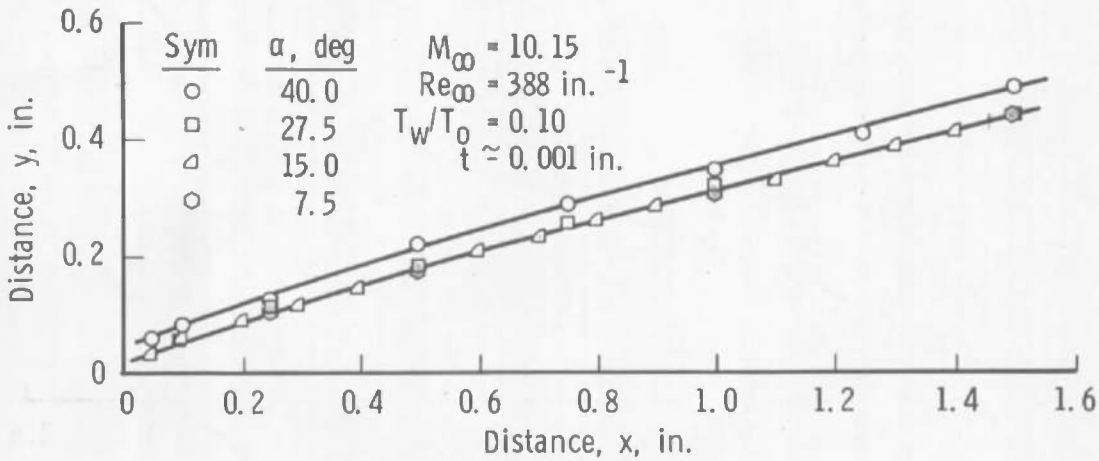

b. Distortion of Profile Peaks Caused by Plate Bevel Angle

Fig. 7 Effects of Bevel Angle and Leading-Edge Thickness

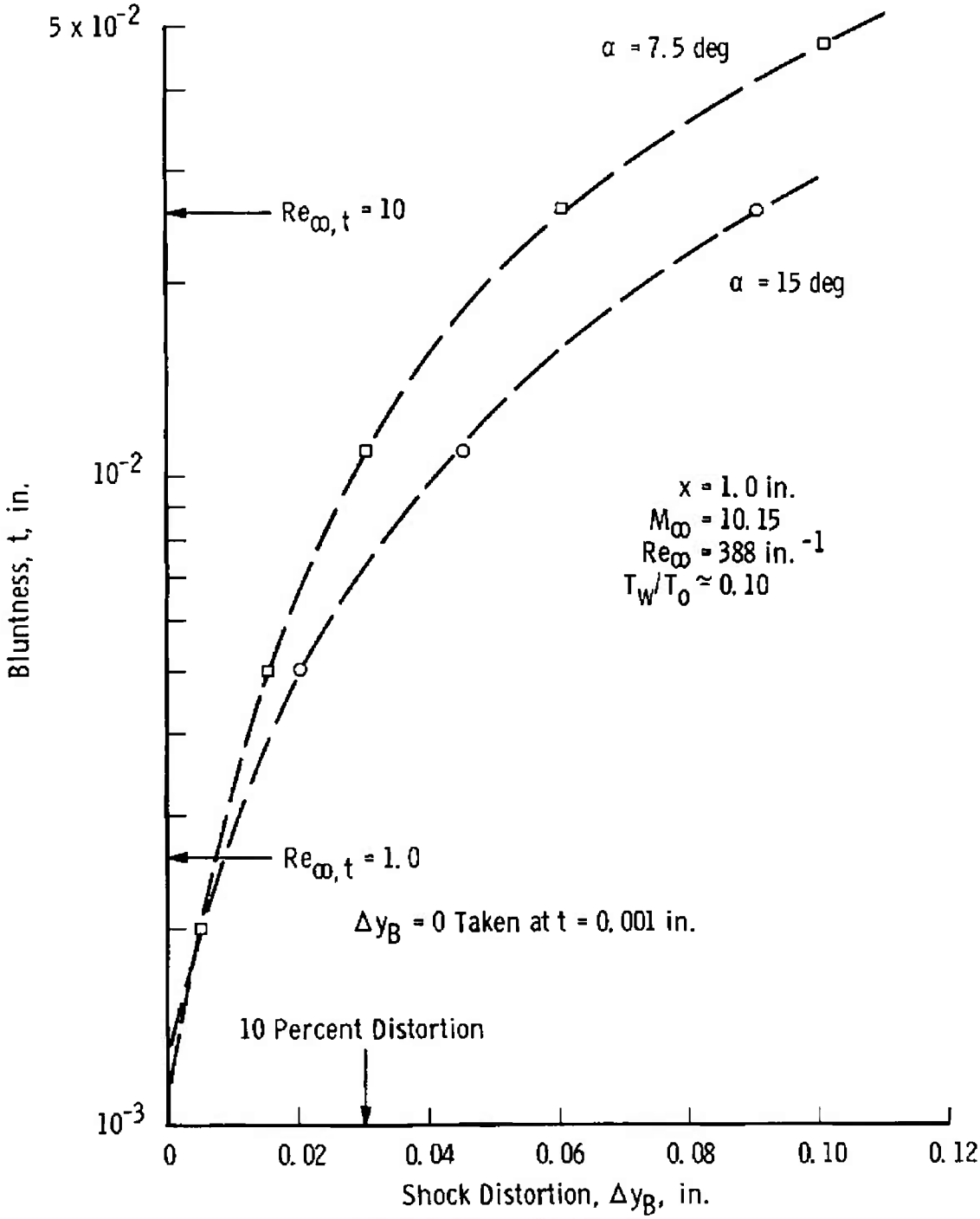

c. Effect of Leading-Edge Bluntness

Fig. 7 Concluded

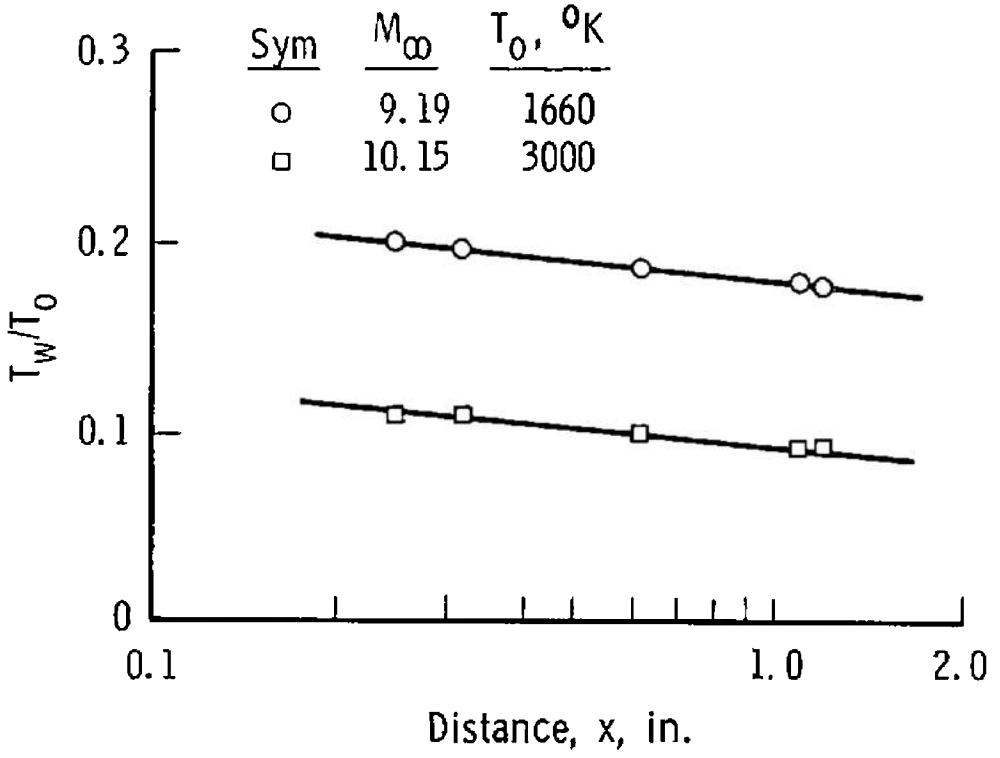

Fig. 8 Model Surface Temperatures

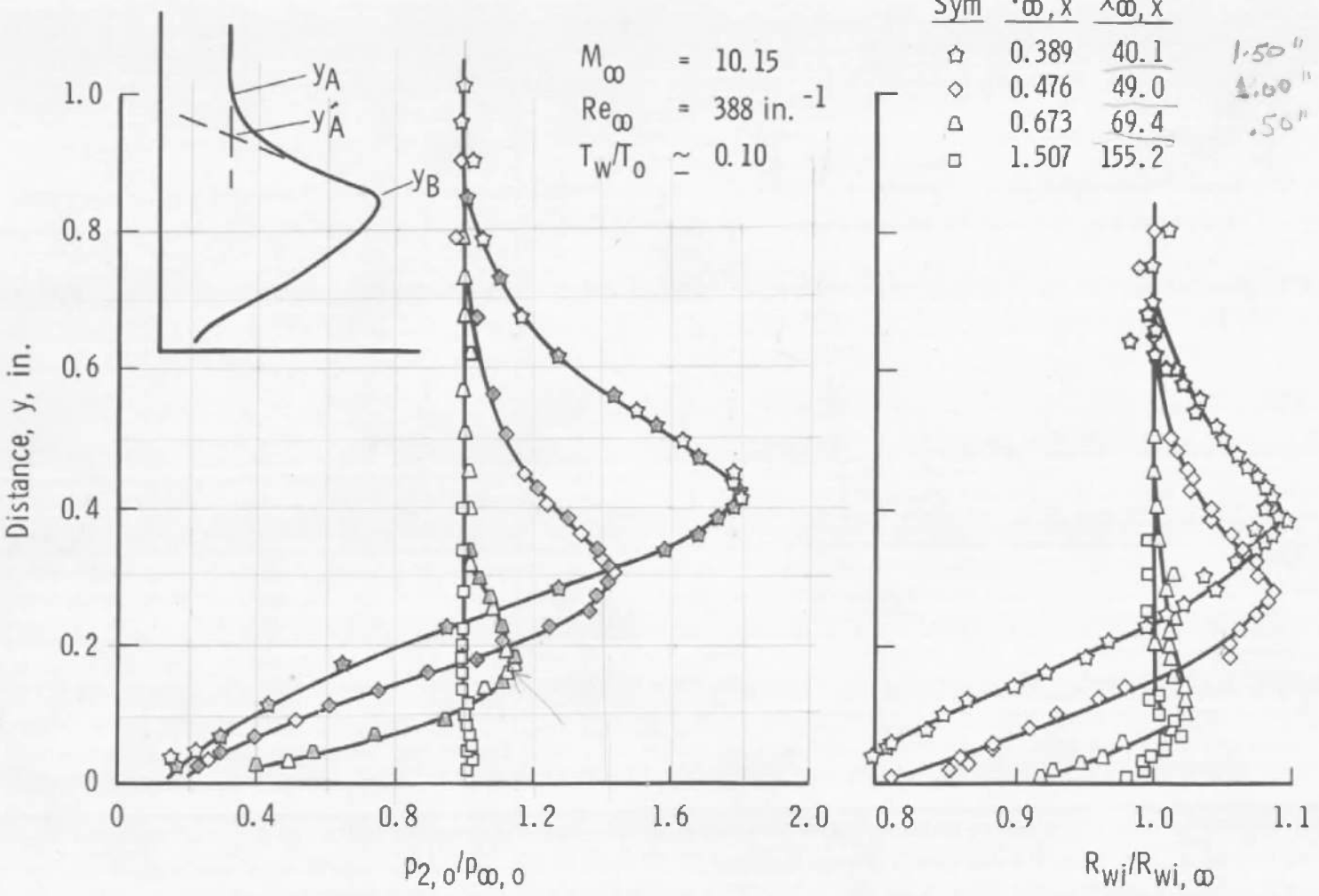

a. Impact Pressures

b. Hot-Wire Measurements

Fig. 9 Flow Field Surveys through the Shock Layer

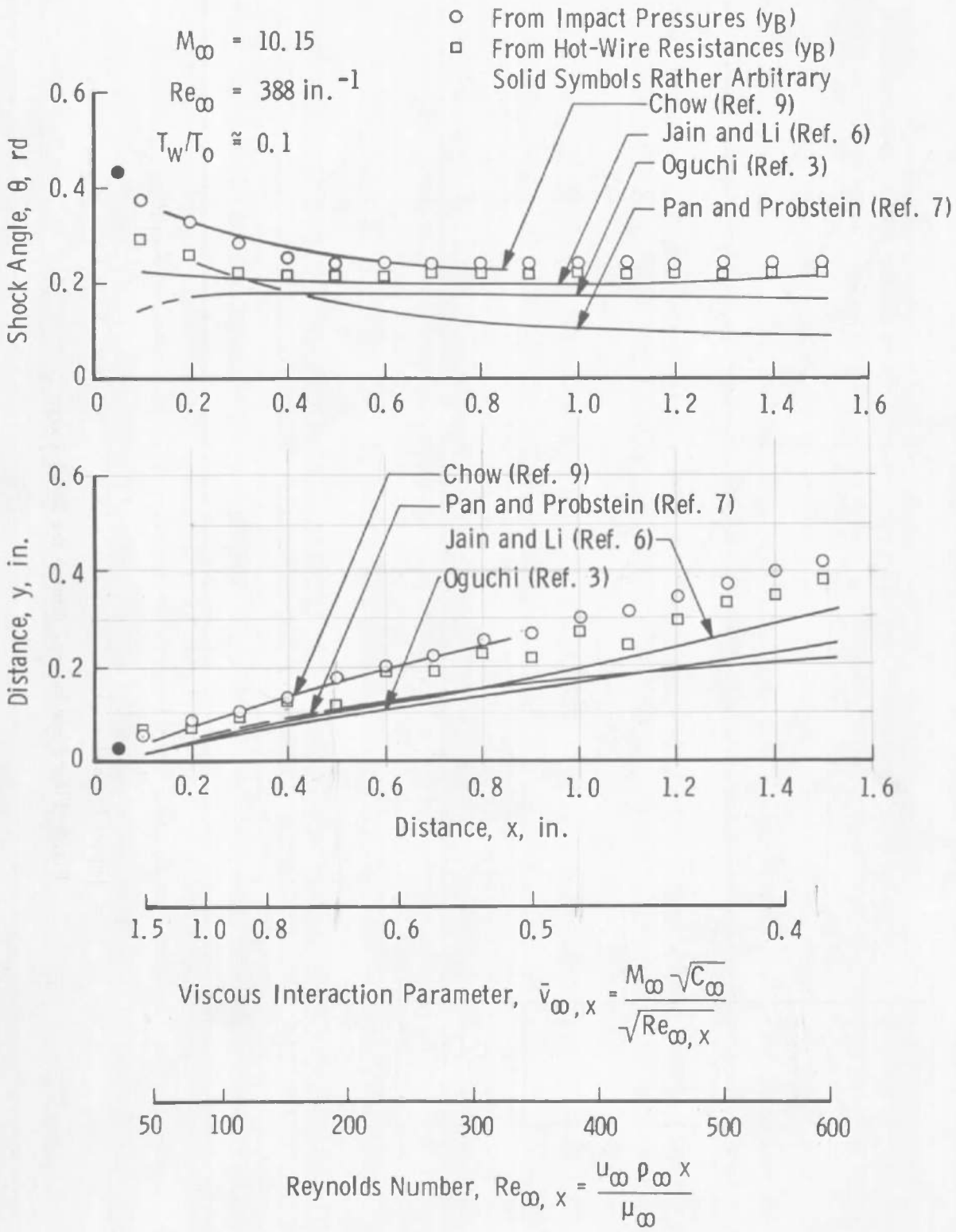

Fig. 10 Profile Peaks and Angles from Impact Pressure and Hot-Wire Resistance Measurements Compared with Theories

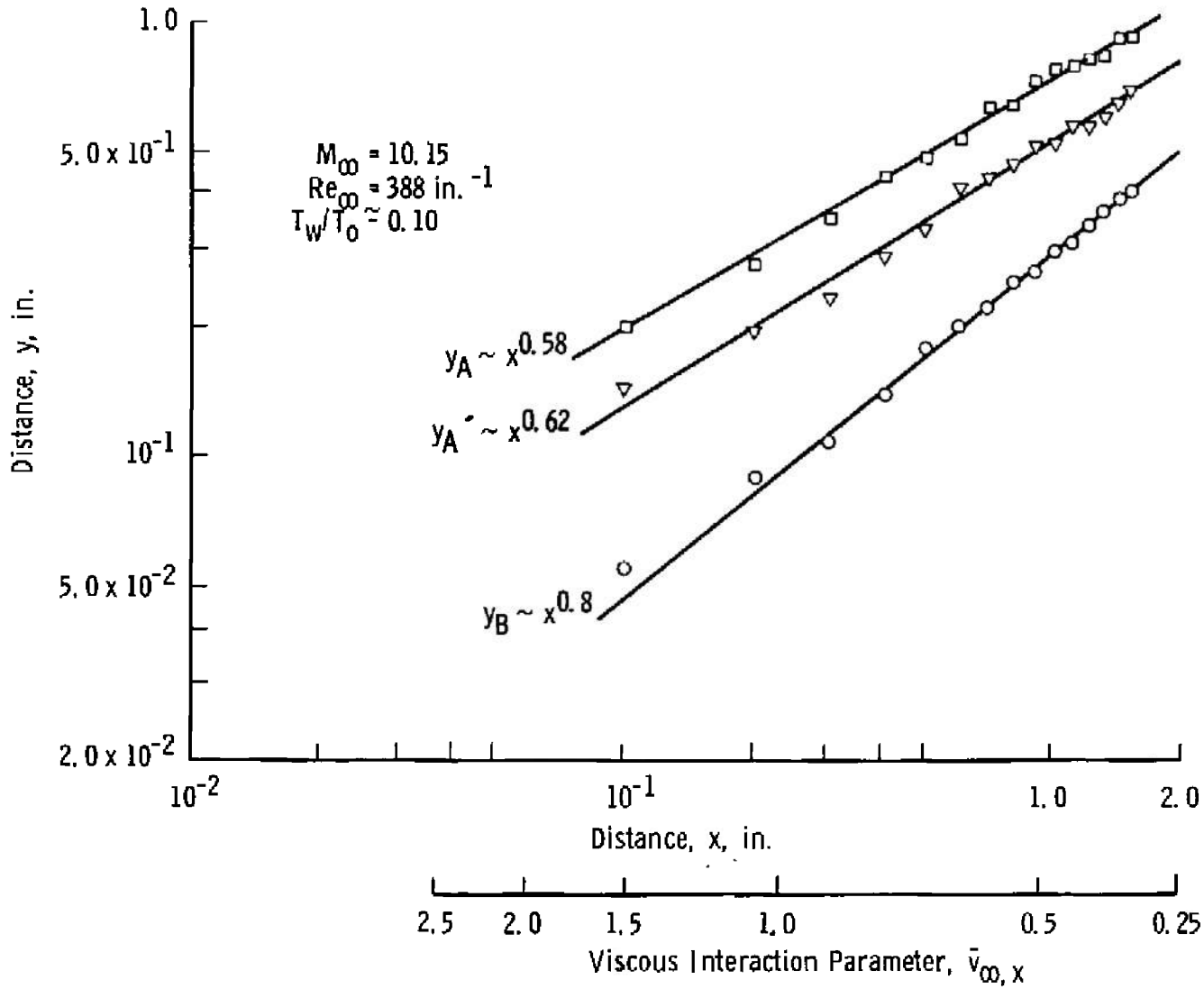

Fig. 11 Shock Layer Thickness and Slope from Impact Pressure Measurements

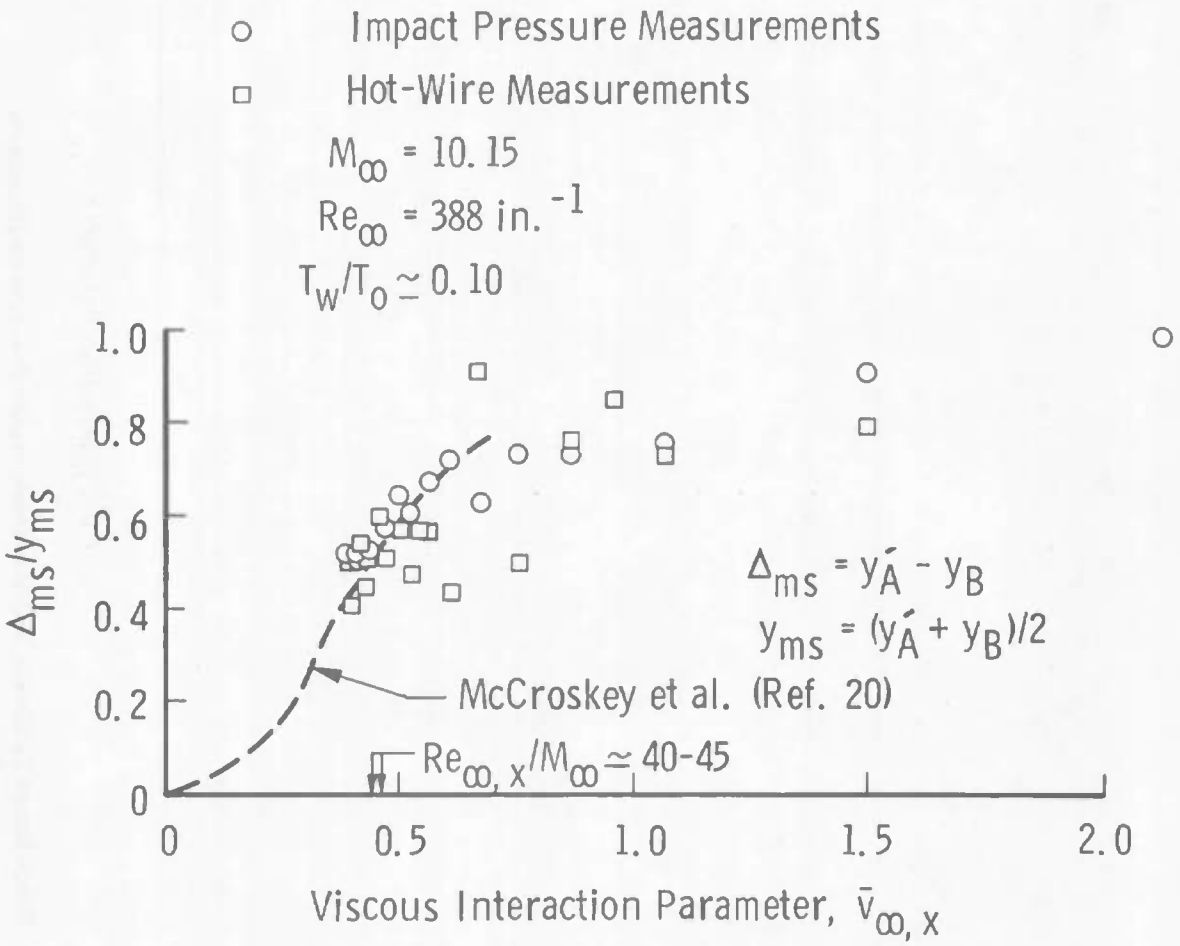

Fig. 12 Shock Wave to Shock Layer Thickness as a Function of the Viscous Interaction Parameter, $\bar{v}_{\infty,x}$

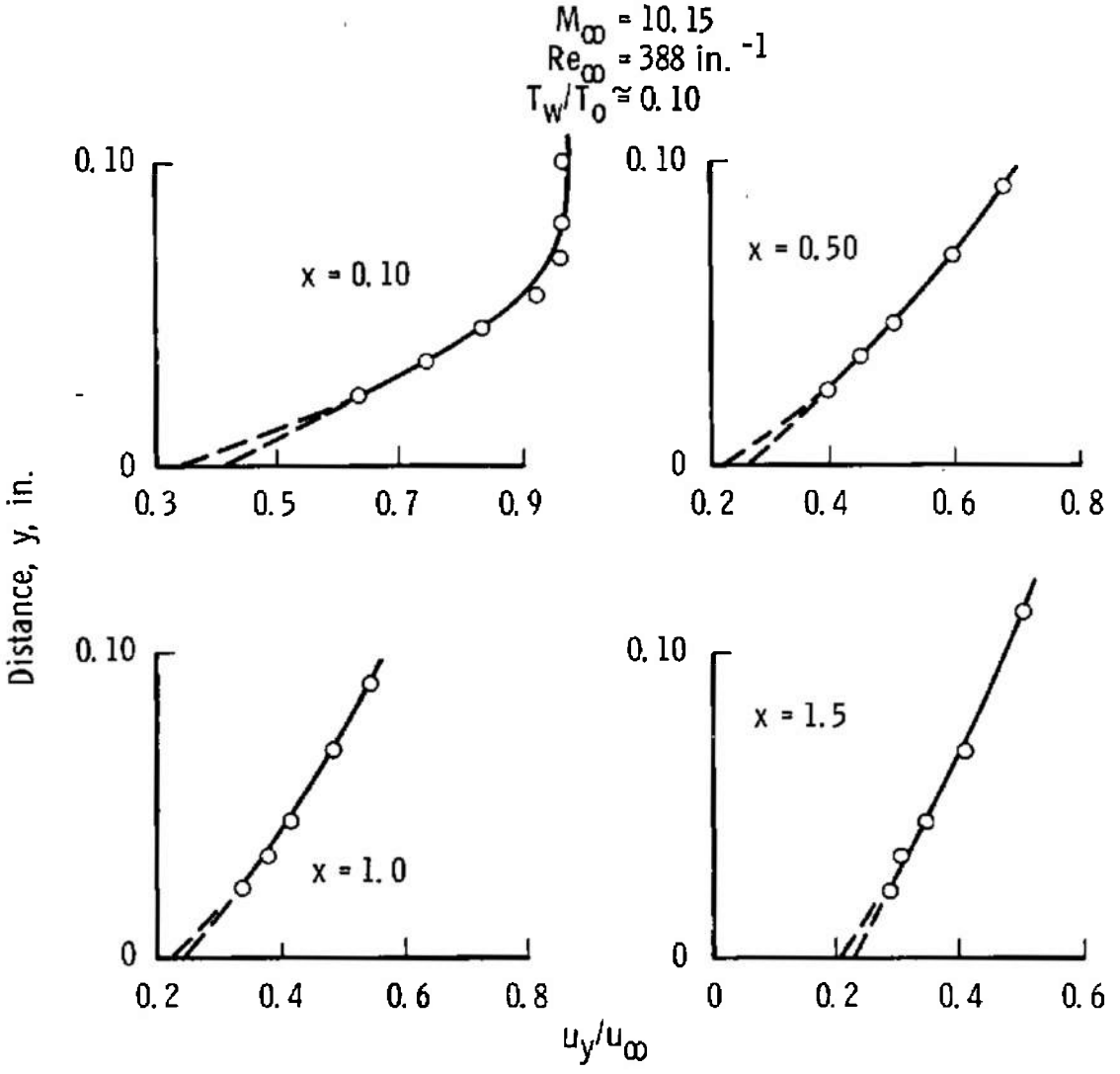

a. Approximate Velocity Profiles

Fig. 13 Calculated Velocity Profiles and Surfact Slip

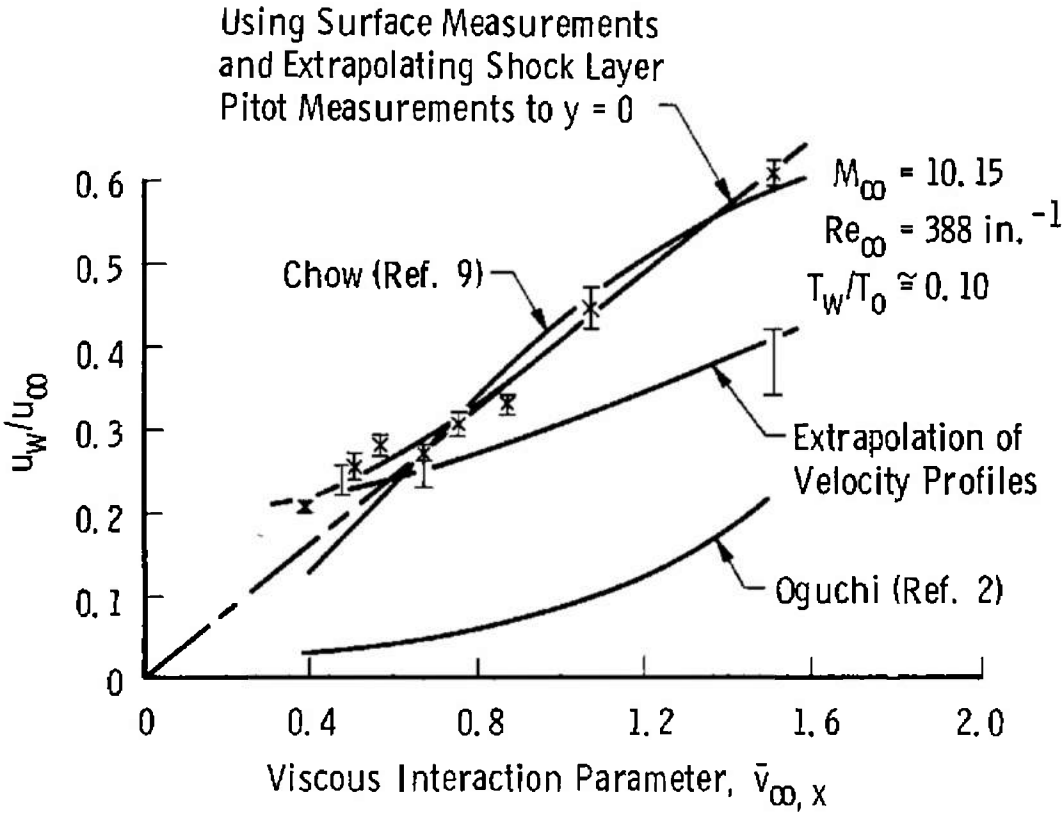

b. Surface Slip Velocity
Fig. 13 Concluded

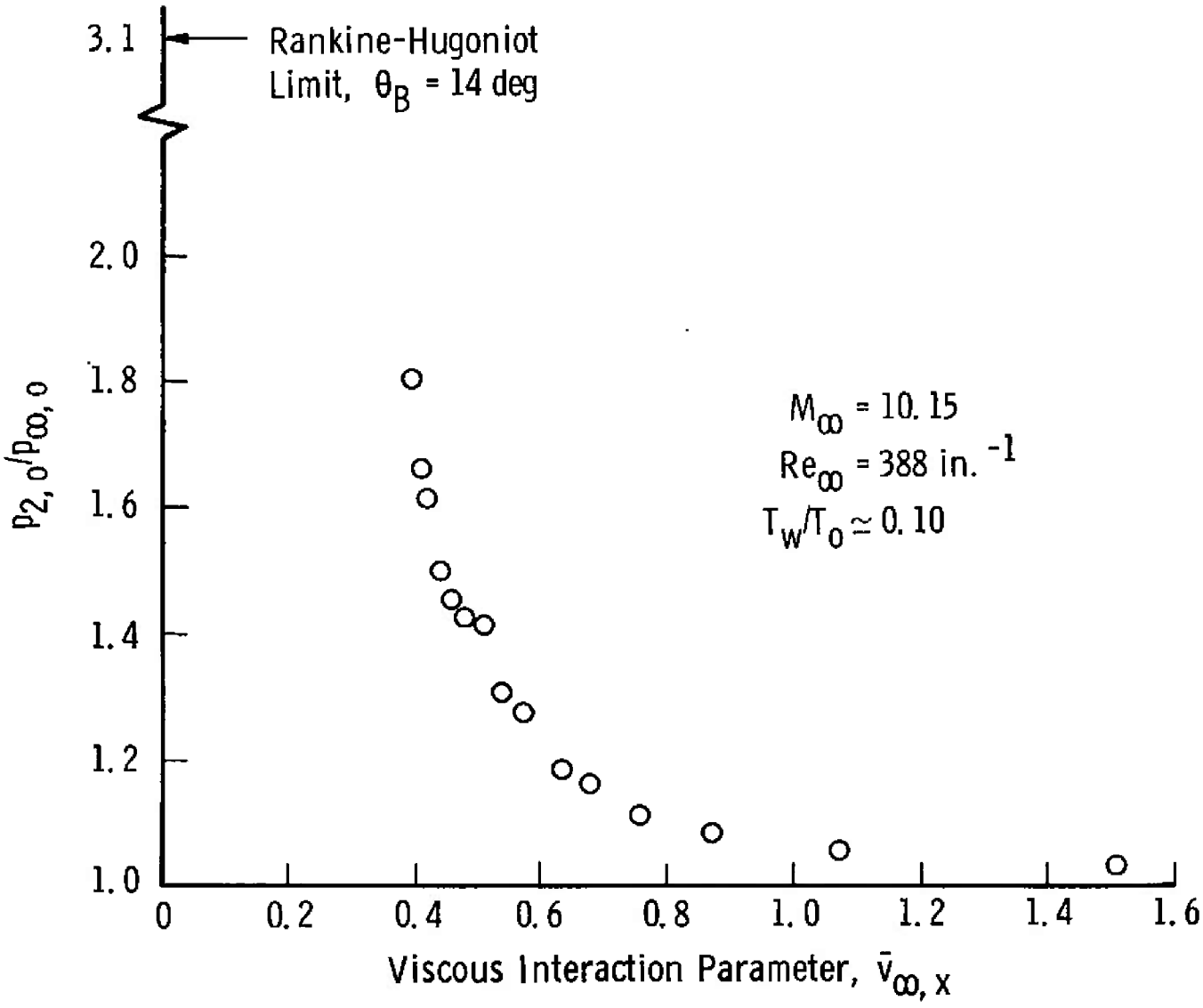

Fig. 14 Apparent Shock Strength as a Function of the Viscous Interaction Parameter, $\bar{v}_{\infty,x}$

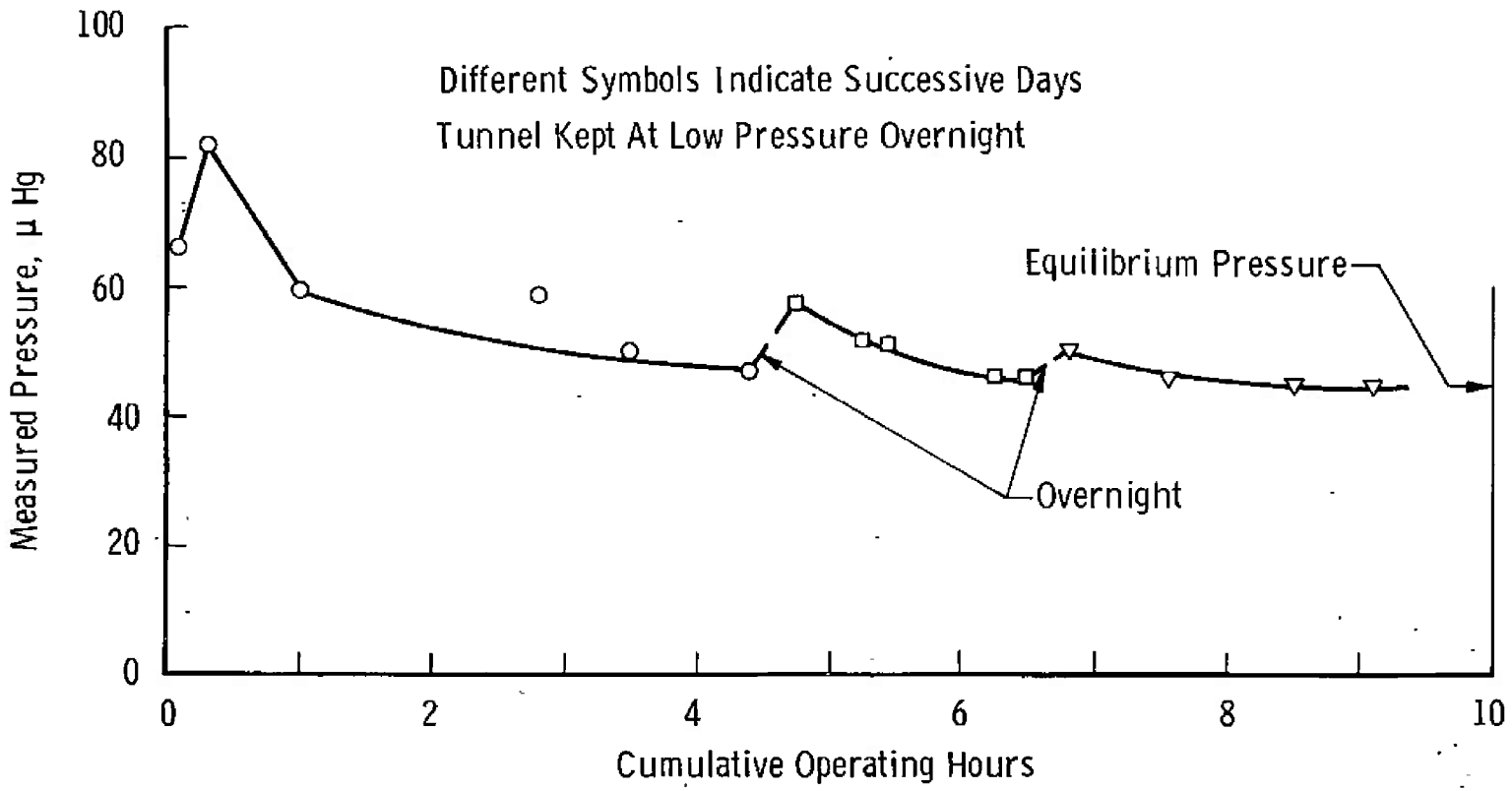

Fig. 15 Typical Surface Pressure Data Acquisition

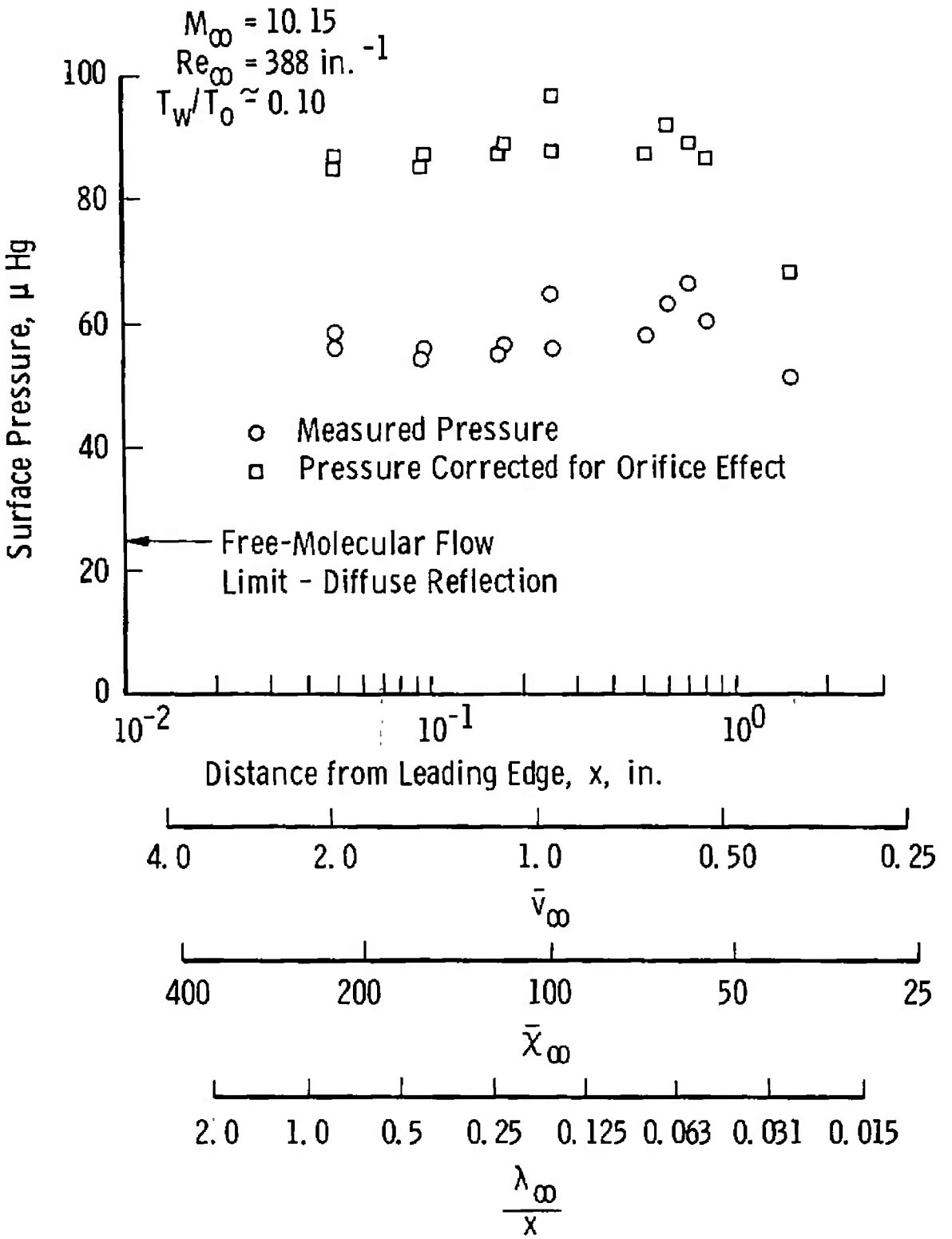

Fig. 16 Typical Surface Pressure Results

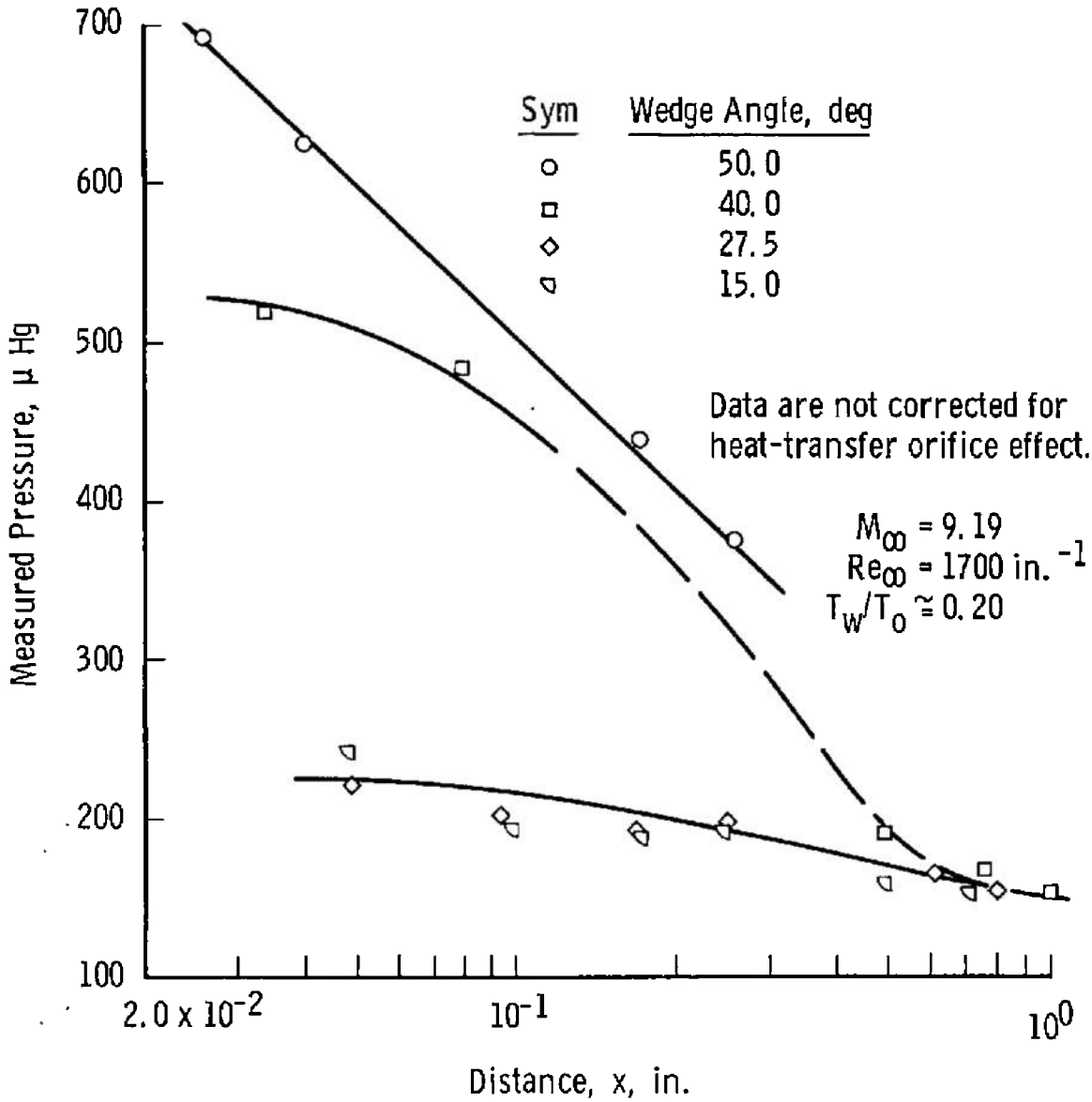

Fig. 17 Effect of Leading-Edge Bevel Angle

Source	Sym	M_∞	Re_∞/in.	T_w/T_o
Nagamatsu et al.	✳	18.5	326	~0.08
(Ref. 18)	+	25.1	7350	0.24
Vidal et al.	◊	20.2	520	0.082
(Ref. 31)*	▽	22.0	1000	0.077
	○	14.7	11400	0.100
Deskins (Ref. 34)	☆	21.2	4700	0.083
	×	21.4	5800	0.083
	⬭	18.7	8300	0.083
Vas et al. (Ref. 33)	D	26.4	13700	0.150
	▽	24.6	6800	0.110
Present Data	●	10.15	388	0.100
	■	9.19	1700	0.200

*Corrected Data as Presented by Garvine (Ref. 8)

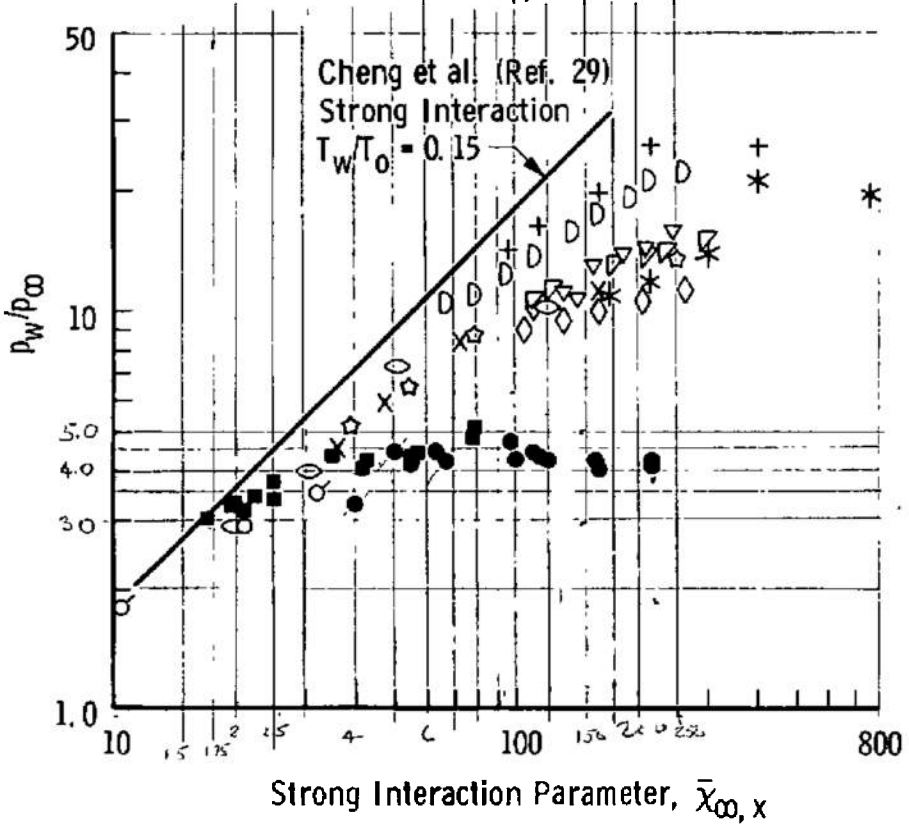

Fig. 18 Available Cold-Wall Flat Plate Surface Pressures in the Merged-Layer Regime

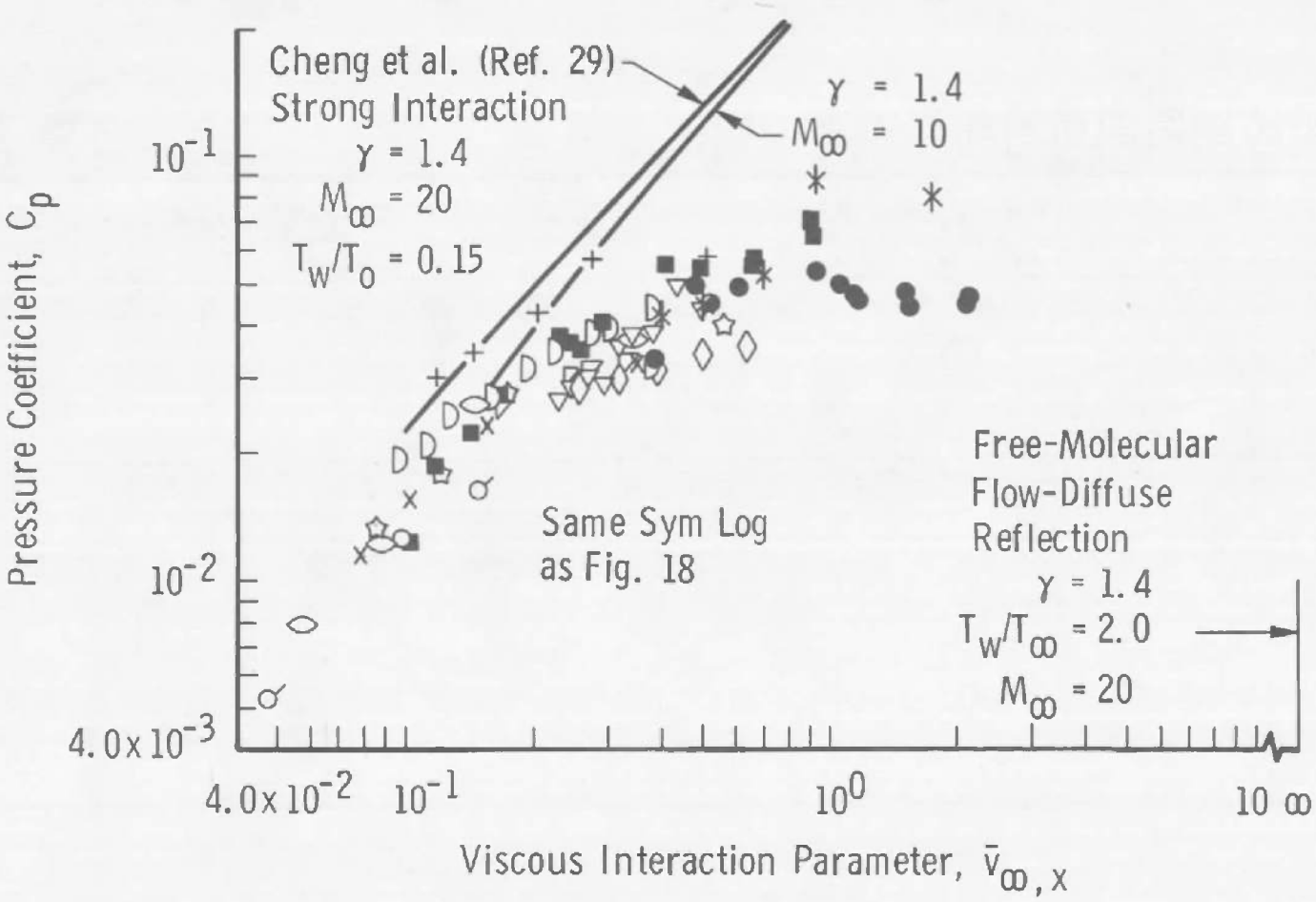

Fig. 19 Correlation of Wall Surface Pressure Distribution

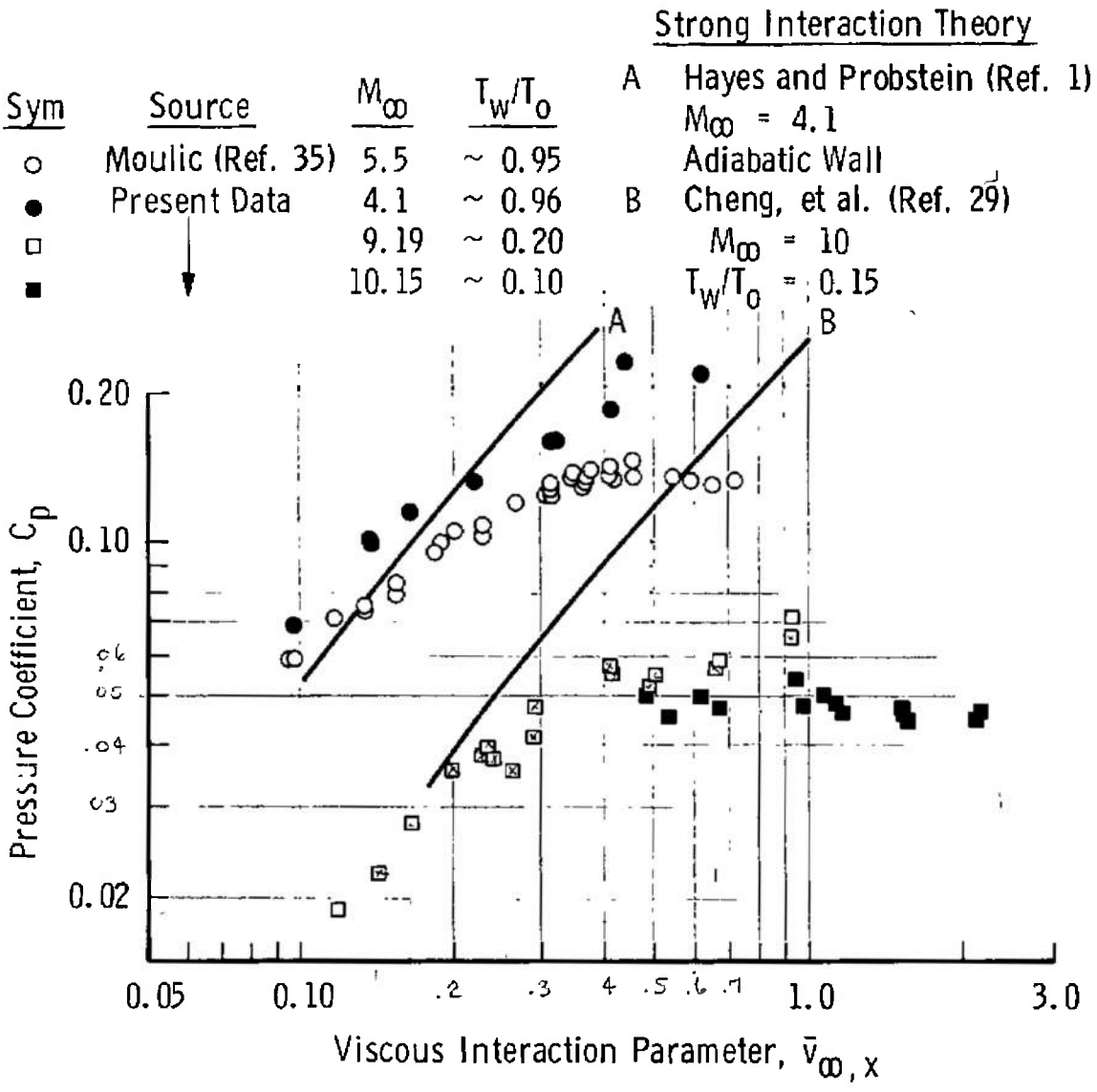

Fig. 20 Effect of Wall Temperature

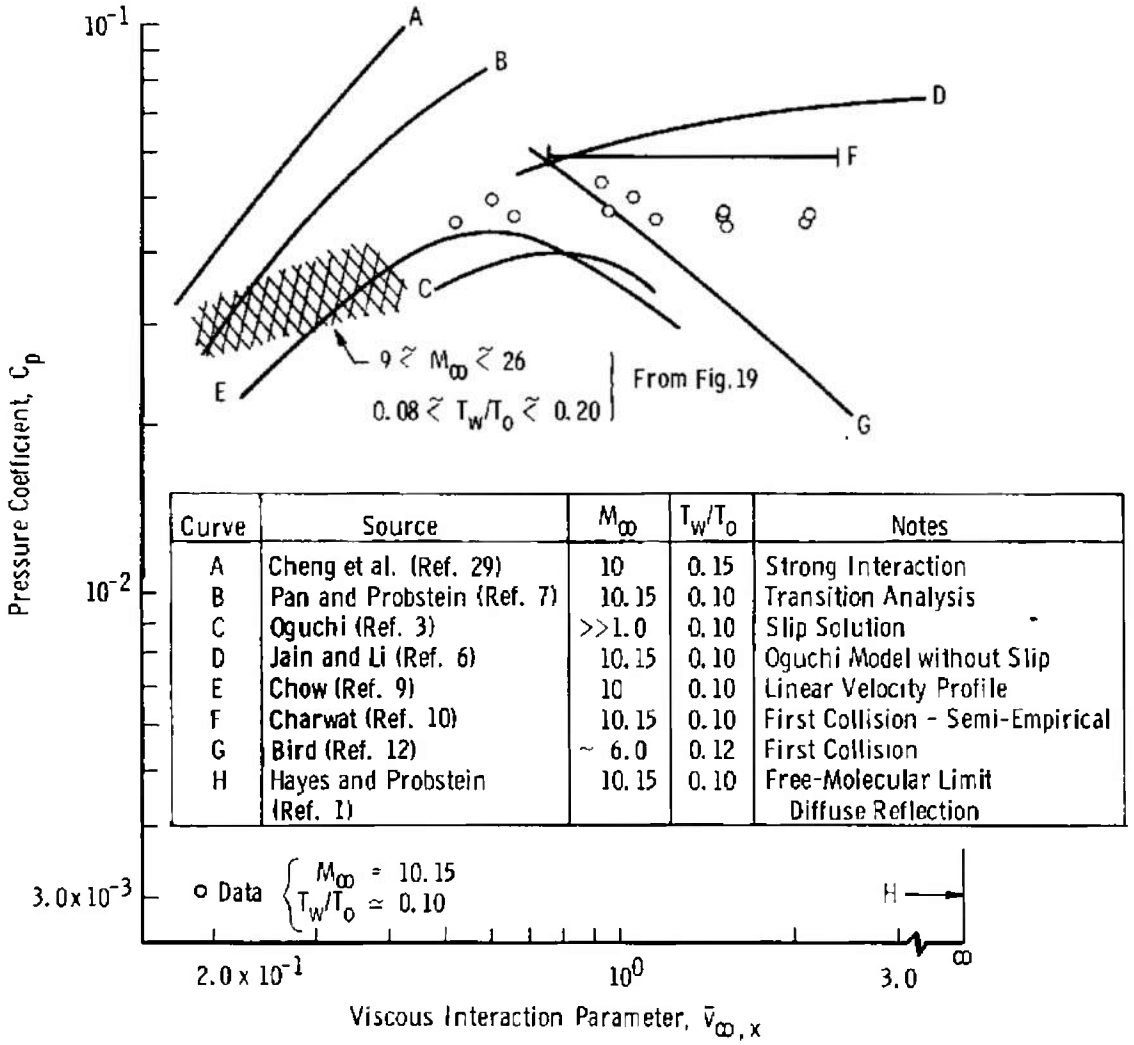

Curve	Source	M_∞	T_w/T_0	Notes
A	Cheng et al. (Ref. 29)	10	0.15	Strong Interaction
B	Pan and Probstein (Ref. 7)	10.15	0.10	Transition Analysis
C	Oguchi (Ref. 3)	>>1.0	0.10	Slip Solution
D	Jain and Li (Ref. 6)	10.15	0.10	Oguchi Model without Slip
E	Chow (Ref. 9)	10	0.10	Linear Velocity Profile
F	Charwat (Ref. 10)	10.15	0.10	First Collision - Semi-Empirical
G	Bird (Ref. 12)	~ 6.0	0.12	First Collision
H	Hayes and Probstein (Ref. 1)	10.15	0.10	Free-Molecular Limit Diffuse Reflection

Fig. 21 Comparison of Available Theoretical Results in the Merged-Layer Regime

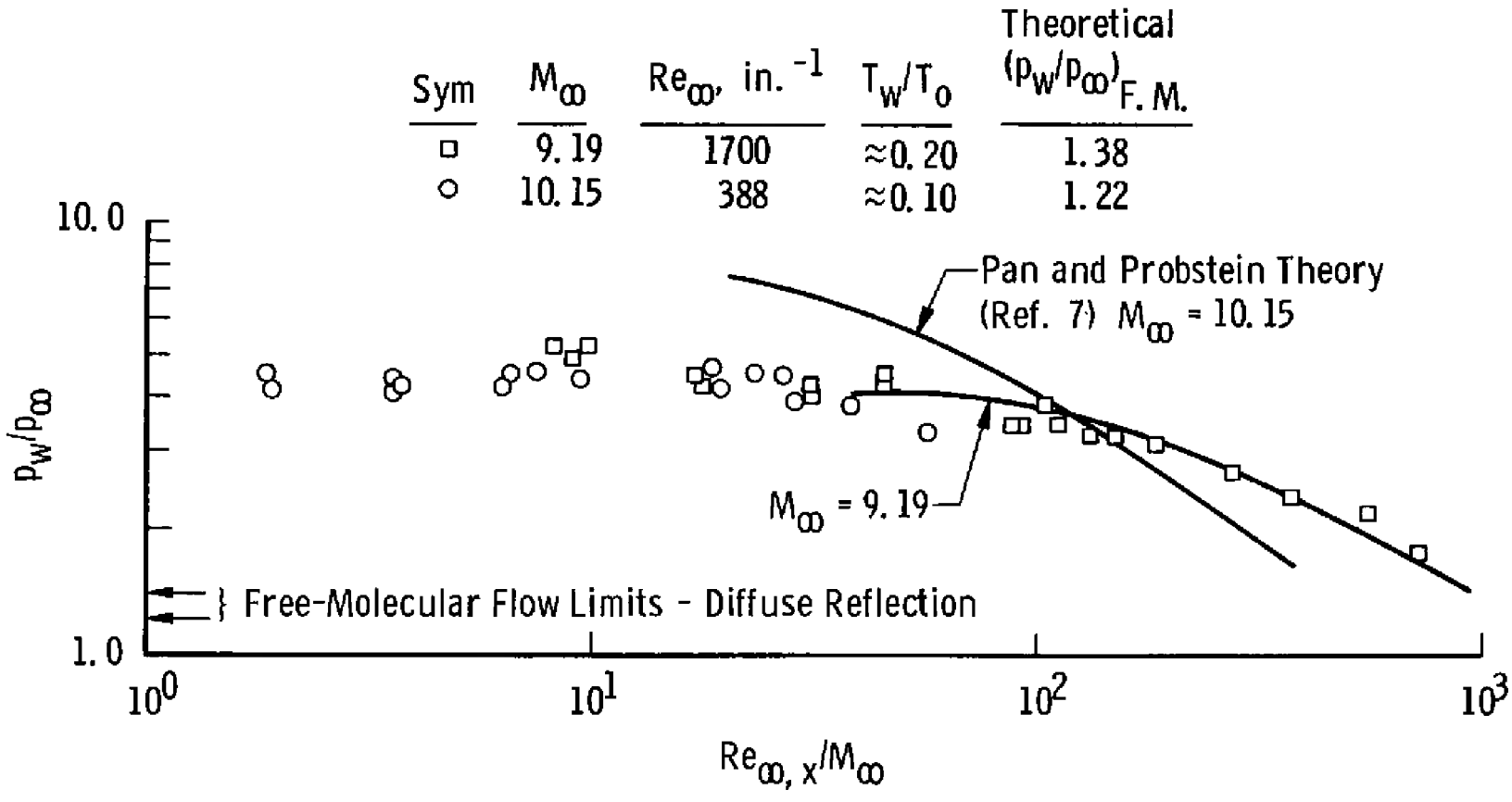

Fig. 22 Surface Pressure Distribution Using Parameter of Pan and Probstein (Ref. 7)

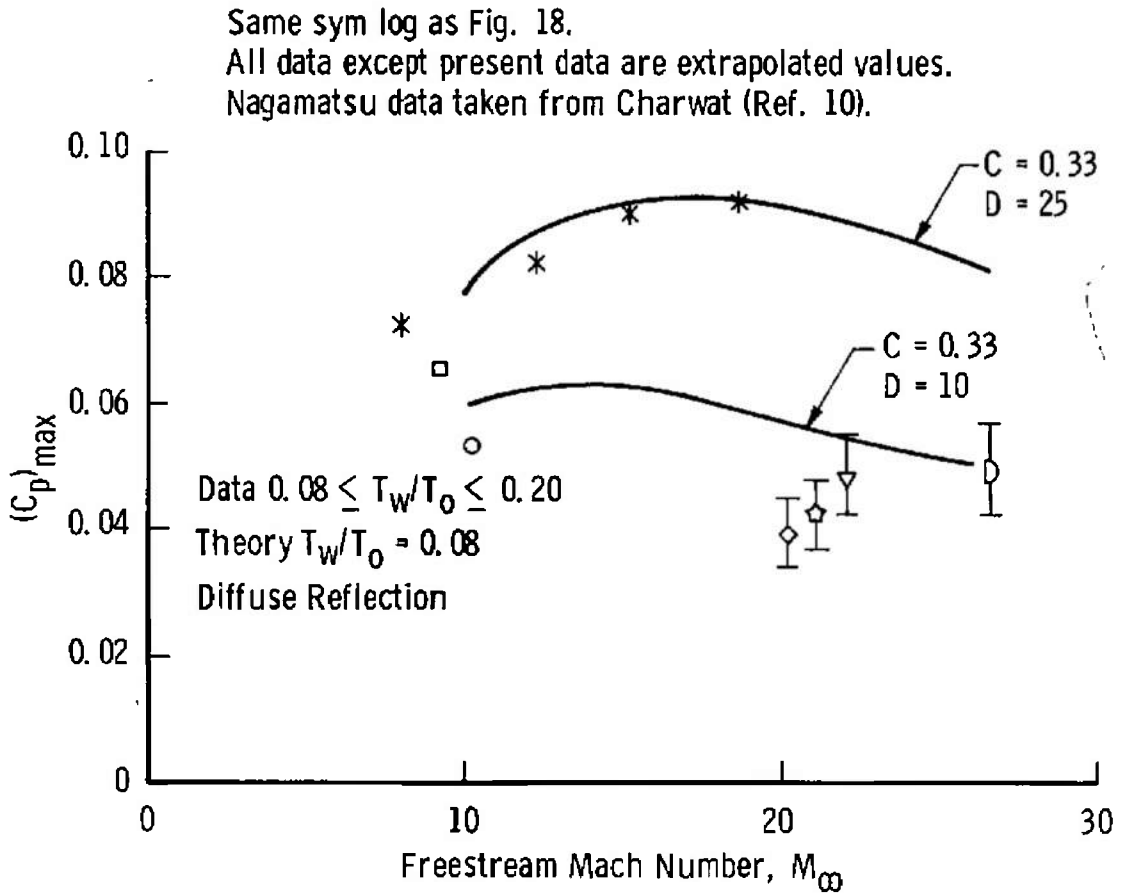

Fig. 23 First Collision Theory of Charwat (Ref. 10) Compared to Available Experimental Results

TABLE I
FLOW CONDITIONS

	Nozzle A	Nozzle B
M_∞	9.19	10.15
p_O, psia	25	18
T_O, °K	1660	3000
p_∞, μ Hg	55	20
T_W, °K	300	300
T_∞, °K	96	144
C_∞	0.817	0.852
Re_∞ in.$^{-1}$	1700	388
λ_∞, in.*	0.008	0.04
$\bar{v}_\infty$, in.$^{1/2}$	0.201	0.476
$\bar{X}_\infty$, in.$^{1/2}$	17.0	49.2

*Based on static billiard ball model.

TABLE II
COLD-WALL PRESSURE DISTRIBUTION STUDIES IN THE MERGED-LAYER REGIME

Source	M_∞	T_W/T_O	Approximate Upper Limit of Rarefaction	
			$\bar{X}_{\infty, x}$	$\bar{V}_{\infty, x}$
Nagamatsu (Ref. 18)	8.0 - 25.1	0.08 - 0.24	760	1.76
Vidal (Ref. 31)	14.1 - 24.0	0.077 - 0.10	260	0.65
Deskins (Ref. 34)*	18.7 - 21.4	0.083	250	0.56
Vas (Ref. 33)	24.0 - 26.4	0.11 - 0.15	300	0.49
Present Study	9.2 - 10.2	0.10 - 0.20	220	2.00

*Excluding Tunnel L data.

Security Classification

DOCUMENT CONTROL DATA - R&D

(Security classification of title, body of abstract and indexing annotation must be entered when the overall report is classified)

1 ORIGINATING ACTIVITY (Corporate author) Arnold Engineering Development Center ARO, Inc., Contract Operator Arnold Air Force Station, Tennessee	2a REPORT SECURITY CLASSIFICATION UNCLASSIFIED 2b GROUP N/A

3 REPORT TITLE

FLOW FIELD AND SURFACE PRESSURE MEASUREMENTS IN THE FULLY MERGED AND TRANSITION FLOW REGIMES ON A COOLED SHARP FLAT PLATE

4 DESCRIPTIVE NOTES (Type of report and inclusive dates)

N/A

5 AUTHOR(S) (Last name, first name, initial)

Becker, Manfred and Boylan, David E., ARO, Inc.

6 REPORT DATE	7a TOTAL NO OF PAGES	7b NO OF REFS
September 1966	58	35

8a CONTRACT OR GRANT NO.	9a ORIGINATOR'S REPORT NUMBER(S)
AF40(600)-1200 b. PROJECT NO 8953	AEDC-TR-66-111
c Program Element 62405334 d Task 895306	9b OTHER REPORT NO(S) (Any other numbers that may be assigned this report) N/A

10 AVAILABILITY/LIMITATION NOTICES Qualified users may obtain copies of this report from DDC. Distribution of this document is unlimited.

11 SUPPLEMENTARY NOTES	12 SPONSORING MILITARY ACTIVITY
Info. presented at 5th Intl. Sym. on Rarefied Gas Dynamics, Oxford, England, July 4-8, 1966	Arnold Engineering Development Center, Air Force Systems Command, Arnold Air Force Station, Tennessee

13 ABSTRACT

The experimental survey of the flow field near the leading edge of a cooled, sharp flat plate parallel to a hypersonic stream of low density is discussed. Results consisting of impact pressure and hot-wire anemometer profiles plus surface pressures are analyzed and compared to recent theoretical results. Data are presented for viscous interaction parameters, $M_\infty (C_\infty/Re_\infty)^{1/2}$, as high as 2.0.

DD FORM 1 JAN 64 1473

Security Classification

14 KEY WORDS	LINK A		LINK B		LINK C	
	ROLE	WT	ROLE	WT	ROLE	WT
flow fields						
flat plates						
surface pressure measurements						
hypersonic flow						
low density						
hot-wire anemometers						
viscous interaction parameters						
transition flow						
fully merged flow						

INSTRUCTIONS

1. ORIGINATING ACTIVITY: Enter the name and address of the contractor, subcontractor, grantee, Department of Defense activity or other organization *(corporate author)* issuing the report.

2*a*. REPORT SECURITY CLASSIFICATION: Enter the overall security classification of the report. Indicate whether "Restricted Data" is included. Marking is to be in accordance with appropriate security regulations.

2*b*. GROUP: Automatic downgrading is specified in DoD Directive 5200.10 and Armed Forces Industrial Manual. Enter the group number. Also, when applicable, show that optional markings have been used for Group 3 and Group 4 as authorized.

3. REPORT TITLE: Enter the complete report title in all capital letters. Titles in all cases should be unclassified. If a meaningful title cannot be selected without classification, show title classification in all capitals in parenthesis immediately following the title.

4. DESCRIPTIVE NOTES: If appropriate, enter the type of report, e.g., interim, progress, summary, annual, or final. Give the inclusive dates when a specific reporting period is covered.

5. AUTHOR(S): Enter the name(s) of author(s) as shown on or in the report. Enter last name, first name, middle initial. If military, show rank and branch of service. The name of the principal author is an absolute minimum requirement.

6. REPORT DATE: Enter the date of the report as day, month, year, or month, year. If more than one date appears on the report, use date of publication.

7*a*. TOTAL NUMBER OF PAGES: The total page count should follow normal pagination procedures, i.e., enter the number of pages containing information.

7*b*. NUMBER OF REFERENCES: Enter the total number of references cited in the report.

8*a*. CONTRACT OR GRANT NUMBER: If appropriate, enter the applicable number of the contract or grant under which the report was written.

8*b*, 8*c*, & 8*d*. PROJECT NUMBER: Enter the appropriate military department identification, such as project number, subproject number, system numbers, task number, etc.

9*a*. ORIGINATOR'S REPORT NUMBER(S). Enter the official report number by which the document will be identified and controlled by the originating activity. This number must be unique to this report.

9*b*. OTHER REPORT NUMBER(S): If the report has been assigned any other report numbers *(either by the originator or by the sponsor)*, also enter this number(s).

10. AVAILABILITY/LIMITATION NOTICES: Enter any limitations on further dissemination of the report, other than those imposed by security classification, using standard statements such as:

(1) "Qualified requesters may obtain copies of this report from DDC."

(2) "Foreign announcement and dissemination of this report by DDC is not authorized."

(3) "U. S. Government agencies may obtain copies of this report directly from DDC. Other qualified DDC users shall request through

_____."

(4) "U. S. military agencies may obtain copies of this report directly from DDC. Other qualified users shall request through

_____."

(5) "All distribution of this report is controlled. Qualified DDC users shall request through

_____."

If the report has been furnished to the Office of Technical Services, Department of Commerce, for sale to the public, indicate this fact and enter the price, if known.

11. SUPPLEMENTARY NOTES: Use for additional explanatory notes.

12. SPONSORING MILITARY ACTIVITY: Enter the name of the departmental project office or laboratory sponsoring *(paying for)* the research and development. Include address.

13 ABSTRACT: Enter an abstract giving a brief and factual summary of the document indicative of the report, even though it may also appear elsewhere in the body of the technical report. If additional space is required, a continuation sheet shall be attached.

It is highly desirable that the abstract of classified reports be unclassified. Each paragraph of the abstract shall end with an indication of the military security classification of the information in the paragraph, represented as *(TS), (S), (C), or (U)*

There is no limitation on the length of the abstract. However, the suggested length is from 150 to 225 words.

14. KEY WORDS: Key words are technically meaningful terms or short phrases that characterize a report and may be used as index entries for cataloging the report. Key words must be selected so that no security classification is required. Identifiers, such as equipment model designation, trade name, military project code name, geographic location, may be used as key words but will be followed by an indication of technical context. The assignment of links, rules, and weights is optional.